Norwegian University
of Life Sciences

Master's Thesis 2018/19 60 ECTS
Faculty of Chemistry, Biotechnology and Food science (KBM)

Detection of fungi with Liquid Array Diagnostics in dysbiotic patients

Zuzanna Gulczynska
MSc Biotechnology, Microbiology

Preface

Not everybody is lucky enough to write their master thesis on the subject that really interests them, yet I have been lucky enough to get my dream project.

I would like to thank professor Knut Rudi, my main supervisor, for giving me this opportunity, for all of the advice and guidance, and for continuous positivity throughout this project.

To Pranvera Hiseni, I can never thank you enough for all your help, time, patience and engagement in this project. Our discussions have been priceless, as they always challenged my way of thinking and helped me develop. Thank you.

A very big thank you goes to Inga and Morten at MiDiv lab, for all their help with practical performance of the project, and for the patience to always answer my questions.

Finally, to my fellow master students: thank you for always being helpful and supportive, and for really making working on this project a pleasant experience.

Ås, May 2019

Zuzanna Gulczynska

Abbreviations

A - adenine

AIEC – adherent-invasive *Escherichia coli*

ASCA – anti-*Saccharomyces cerevisiae* antibodies

BLAST – Basic Local Alignment Search Tool

BMI – body mass index

CD – Crohn's disease

C - cytosine

CFU – colony forming unit

CNS – central nervous system

ddCTP – dideoxycytidine triphosphate

ddPCR – droplet digital polymerase chain reaction

DI – Dysbiosis Index

DNA – deoxyribonucleic acid

dNTP – deoxyribonucleoside trophosphate

ENS – enteric nervous system

FN – false negative

FP – false positive

G - guanine

GA – Genetic Analysis

GA-map – Genetic Analysis microbiota array platform

gDNA – genomic deoxyribonucleic acid

IBD – inflammatory bowel disease

IBS – irritable bowel syndrome

IBS-C – IBS with predominant constipation

IBS-D – IBS with predominant diarrhea

IBS-M – IBS with predominant mixed bowel habits

IgA – Immunoglobulin A

IgG – Immunoglobulin G

ITS – Internal transcribed spacer

LAD – Liquid Array Diagnostics

LP – labelling probe

LPS – lipopolysaccharide

NGS – next generation sequencing

NLR – NOD-like receptor

PAMP – pathogen-associated molecular patterns

PCR – polymerase chain reaction

PRR – pattern recognition receptor

rDNA – ribosomal deoxyribonucleic acid

ROC – receiver operating characteristic

RP – reporter probe

rRNA – ribosomal ribonucleic acid

SCFA – short chain fatty acids

SDS – sodium dodecyl sulfate

SFB – segmented filamentous bacteria

SOLiD – Sequencing by Oligonucleotide Ligation and Detection

T - thymine

TAE – Tris-acetate-EDTA

TLR – toll-like receptor

Tm – melting temperature

TN – true negative

TP – true positive

UC – ulcerative colitis

VB – vagus nerve

Sammendrag

Tarmmikrobiota dysbiose forbindes med diverse medisinske tilstander, inkludert inflammatorisk tarmsykdom (IBD) og irritabel tarmsyndrom (IBS). Som følge av mange år med omfattende forskning innen tarmmikrobiota, er noen bakterier i dag assosiert med dysbiose, mens andre er assosiert med normobiotisk tilstand. Disse assosiasjoner var grunnlaget til utviklingen av GA-map® Dysbiosis Test – et probe-basert diagnostisk verktøy for bestemmelse av dysbiosenivå, oppgitt som Dysbiose Index (DI). En ny teknologi, Liquid Array Diagnostics (LAD), er under utvikling for å utfylle GA-map® Dysbiosis Test, med hensyn til dets tilgjengelighet og kostnadseffektivitet. De siste årene har studier tilknyttet tarmmikrobiota blitt utvidet til å fokusere på andre mikroorganismer som er tilstede i tarmen, blant annet fungi. I noen studier har det blitt rapportert at dysbiose-relaterte mønstre kan observeres også blant tarmmycobiota. Disse mønstrene inkluderer skjev Basidiomycota/Ascomycota ratio, økt andel av *Candida albicans* og redusert andel av *Saccharomyces cerevisiae*. Målet med denne studien var å identifisere mycobiotas sammensetning i avføringsprøver med forskjellige DI, og å evaluere utvalgte fungi som potensielle mål for LAD-prober. For å oppnå dette ble mikro- og mycobiota av 43 avføringsprøver kvantifisert og identifisert ved hjelp av Illumina sekvensering. Sekvenseringsresultatene ble benyttet til å evaluere assosiasjoner mellom fungi og dysbiosenivå. 10 målorganismer var utvalgt til LAD-probe design. LAD ble så utført på de originale 43 avføringsprøvene, og sekvenseringsresultatene ble benyttet. Til tross for at ingen taksonomiske mønstre assosiert med dysbiose ble identifisert, ble alle målorganismer detektert ved bruk av LAD. Det var et godt samsvar mellom LADs nøyaktighet og Illumina sekvensering. LAD har et stort potensial til bruk i klinisk sammenheng. Imidlertid behøves det flere studier til å identifisere og bekrefte dysbiose-assosierte fungi, før prober rettet mot fungi kan inkluderes i en LAD-dysbiose analyse.

Abstract

Gut microbiota dysbiosis is connected with various medical conditions, including inflammatory bowel disease (IBD) and irritable bowel syndrome (IBS). Years of extensive research on gut microbiota revealed many bacterial taxa which are indicative of dysbiosis or normobiosis. These findings lead to development of GA-map® Dysbiosis Test, a diagnostic tool for assessment of the degree of dysbiosis expressed as Dysbiosis Index (DI), based on probes targeting different bacterial taxa. A new technology, Liquid Array Diagnostics (LAD), is in development and aims to complement GA-map® Dysbiosis Test in terms of cost-effectivity and availability. In recent years, the focus of microbiota studies has been shifted to also examine other microorganisms, such as fungi. A number of studies reported that certain mycobiota patterns can be observed in dysbiotic samples, including skewed Basidiomycota/Ascomycota ratio, increased *Candida albicans* proportion and decreased *Saccharomyces cerevisiae* proportion. The aim of this study was to identify mycobiota composition in a set of faecal samples of various DI and assess fungi as potential probe targets for LAD. The micro- and mycobiota of 43 faecal samples was first quantified and then identified through Illumina sequencing. Sequencing results were examined for fungal associations with dysbiosis, and 10 targets were chosen for designing of LAD probes. LAD analysis was performed on the same 43 samples using Illumina results as control. Although no taxonomic patterns associated with dysbiosis were found, all targets were successfully detected with LAD. The accuracy of LAD analysis also showed good compliance with Illumina. Although LAD shows a great potential for use in clinical context, more studies are needed to identify and confirm fungal taxa associated with dysbiosis before any fungal targets can be included in the assay.

Table of contents

1. Introduction

1.1 The gut microbiota

The human intestine is colonized by a great variety of microorganisms, together forming the gut microbiota. The gut microbiota consists in big part of bacteria, but it also includes viruses (such as bacteriophages), protea and fungi. The symbiotic character of the gut microbiota, developed over the course of millions of years of evolution, is reflected by its multiple functions. The interaction of the gut microbes with the host is facilitated by metabolites synthetized by the microbes, which can act locally or have a systemic effect. The guts own enteric nervous system (ENS) relies on the various metabolites to regulate the gut functions such as secretion, nutrient intake, or motility. Some regulatory compounds make their way to the central nervous system (CNS) and thus play a role in other processes. In fact, the microbiota communicates with the brain in other ways as well. The vagus nerve (VN) is a core pathway of the signal transmission, with its afferent fibers leading signals to the CNS upon microbial stimulation. In turn, the action of efferent fibers executes the inflammatory reflex, leading to reduction of intestinal inflammation and permeability. Neuroactive compounds released by the microbes can also work on the CNS, reaching the brain through blood. (Bonaz et al., 2018) The extent of the connections between the gut microbiota and the rest of the body reflects the importance of a healthy functioning microbial community for a healthy overall body function. Consequently, the effect of gut microbiota function is not only limited to the gut but can have an impact on other organs as well.

1.1.1 Composition and development

The microbiota has evolved to exist in symbiosis with the human host and is today one of the most eagerly studied aspects of human health. The colonization of the gut is a key process playing crucial role in hosts metabolism and development of immune defense. The colonization process, which is believed to start during birth, is vulnerable to disruptions caused by various factors such as host genetics, mode of delivery, breast milk intake, sanitary conditions, and antibiotics intake. Alterations to the gut microbiota composition imposed by those factors have been shown to increase the risk of developing various diseases later in life. (Rodriguez et al., 2015) At approximately the age of 3 the gut microbiota is considered to be fully developed and reaches a relative equilibrium state. This state of a relative compositional stability can last over long periods of time, but in the same time is a subject of alterations by both external and internal factors. (Rodriguez et al., 2015) (Gentile and Weir, 2018) Changes

in diet, psychological and physical stress, surgery or antibiotic treatment can induce a shift in the balance, causing dysbiosis.

The adult bacterial gut microbiota is dominated by two phyla: Firmicutes and Bacteroidetes, which make up 90% of the gut microbiota. Only a few other phyla are represented, including Actinobacteria, Proteobacteria, Fusobacteria and Verrucomicrobia. (Rinninella et al., 2019) These phyla account for approximately 160 different bacterial species that can be found in fecal samples. (Rodriguez et al., 2015) An extensive study by Li et. al. using data obtained by 16s rRNA gene sequencing projects, such as MetaHit and Human Microbiome Project, aimed to collect a more detailed insight in the gut microbiota composition and provides some clues to the subject of species diversity. Even though the identified species were limited, the 16s rRNA gene sequencing revealed a remarkable number of genes: 9 879 896 genes retrieved from 249 new samples and 1018 earlier published samples. (Li et al., 2014a) This suggests a highly developed functional redundancy, further implying that a relative lack of taxonomic diversity is overshadowed by microbial functional diversity. It is currently believed that the functional diversity, and not the taxonomical diversity is key to a healthy gut microbiota.

Less studied fungal microbiota has gained more interest in the recent years. Fungi are generally not as abundant as bacteria, ranging from 10^2 to 10^6 CFU g^-1 fecal sample. (Scanlan and Marchesi, 2008) A few studies attempted to identify the gut mycobiota of healthy individuals. (Hoffmann et al., 2013) (Dollive et al., 2012) Some common findings were that the gut mycobiota is dominated by members of either Ascomycota or Basidiomycota taxa. The most prevalent fungal species found in the gastrointestinal tract is *Candida* (40% prevalence), while other species found included *Saccharomyces*, *Aspergillus*, *Cryptococcus*, *Penicillium*, and *Pneumocystis*. (Dollive et al., 2012) In a more recent study by Schei et. al. development of the gut mycobiota and mother-offspring transfer were examined. Fungi were detected in fecal samples of majority of the mothers and children, and the children's mycobiota increasingly resembled that of mother's with age. The most abundant species found in both mothers and children over 1 year was *Saccharomyces cerevisiae*, while *Debaromyces hansenii* dominated the mycobiota of children from 10 days to 3 months. (Schei et al., 2017)

1.1.2 Maintenance of the gut barrier function

Living in the close proximity, the interaction between gut microbiota and human cells in the gut is unavoidable. This interaction is in normal condition kept in homeostasis, forming the gut barrier – a frontline for protecting the organism from potential pathogens. Among other mechanisms, the gut barrier depends on the composition and thickness of mucus layer to be

able to perform its function. The gut microbiota plays an important role in keeping the mucus barrier in optimal condition. Mucus itself is composed of mucins – glycoproteins secreted by the goblet cells of the intestinal epithelium. Their product forms a physical barrier that compartmentalizes the microbiota and shields the epithelium. (Wells et al., 2017) Therefore the composition of the mucosa-associated microbiota is different from that associated with lumen. Some microorganisms, such as segmented filamentous bacteria (SFB), are associated with the epithelium, stimulating its immune-secretory function. (Thursby and Juge, 2017) Other bacteria with mucus-modulating abilities are closely associated with the mucus layer, where they can influence its thickness and composition. For instance, *Bacteroides thetaiotaomicron* has been observed to promote goblet cell differentiation and mucin synthesis, while *Faecalibacterium prausnitzii* is thought to reduce this effect. (Wells et al., 2017)

The gut barrier homeostasis is fragile and susceptible for external factors. Simple dietary changes restricting microbiota-accessible carbohydrates may lead to over-grazing of mucus. For some bacteria that normally use dietary glycoproteins as energy source, the mucus can become an alternative source upon unavailability of the usual energy source. (Gentile and Weir, 2018) As a consequence of disrupted gut barrier function, the permeability of the barrier is increased leading to immune-inflammatory response. (Kho and Lal, 2018)

1.1.3 Microbiota and host immunity

During the first few years of life the development of the immune system takes place in the same time as the establishment of gut microbiota. The two processes are tightly interconnected and dependent on each other. As the gut lumen is a frontier where the host cells face countless microorganisms and potential pathogens, it also harbors what is probably the largest collection of immune cells in the human body. The recognition and regulation of commensal versus pathogenic agents is facilitated through pattern recognition receptors (PRRs), such as toll-like receptors (TLRs) or NOD-like receptors (NLRs) located extra- and intracellularly. (Cani, 2018) These receptors are able to detect specific structures, known as pathogen-associated molecular patterns (PAMPs) present on or inside of the pathogenic cells. For example, fungal PAMPs recognized by the immune cells are typically cell wall components, such as chitin, mannan, or beta-glucan. (Huseyin et al., 2017) The interconnection of the gut colonization and the immune system development is illustrated by the case of germ-free mice, in which the development of myeloid and lymphoid progenitor cells is suppressed in the absence of gut microbiota. However, this effect is reversed upon gut microbiota colonization. (Kho and Lal, 2018) Furthermore, both the adult immunity and the

composition of the gut microbiota seem to be dependent on early interactions between the first colonizers and the innate immune system. The IgA immunoglobulins acquired through breast milk recognize and bind microbial antigens, preventing immune activation. In similar way, IgA secreted intestinally later in life perform the same function. (Tomkovich and Jobin, 2016) Some genetic factors are also thought to influence the interactions. A type of PRR called Dectin-1 is involved in identification of beta-glucan in fungal cell wall. However, a polymorphism in the gene coding for Dectin-1 is linked to development of a severe form of ulcerative colitis (UC), caused by an altered response to beta-glucan. In this case, the receptor binding causes an inflammatory response that targets commensal species. (Huseyin et al., 2017) Interestingly, the microbiota can partially control its composition by modulating the levels of specific fecal IgA. For example, *Sutterella* species regulates the levels of fecal IgA by degrading the IgA secretory component. This may play a role for example in regulation of Proteobacteria levels, which are normally high in newborns, but are associated with disease in adults. (Tomkovich and Jobin, 2016)

Less is known about the interactions of mycobiota with the immune system, as most studies that have been done focus on immune-suppressed patients. However, it is important to note that just as bacteria participate in "training" of the hosts immune system, early exposure to fungal beta-glucan has been shown to cause macrophages to stimulate certain epigenetic alterations that cause better response to fungal infections later in life. (Quintin et al., 2012) Primary focus of mycobiota studies has been on *Candida*, which because of its high prevalence is probably the most common opportunistic pathogen and causational agent of mycosis (fungal infection). *Candida albicans* is particularly dangerous in immunocompromised patients, where it can cause severe reactions. By stimulating the immune cells *Candida albicans* can induce pro-inflammatory cytokine production, as well as proliferation and apoptosis of epithelial cells. (Tomkovich and Jobin, 2016) Most notably premature and underweight neonates are considered a risk group for acquiring extensive and potentially life-threatening fungal infections, with one study reporting a remarkable high diversity of fungal species in 64% of individuals in this particular group. (LaTuga et al., 2011)

1.1.4 Microbiota and host metabolism

The microbiotas interaction with the immune system is closely connected to host metabolism. While microbial function provides the host with some vital metabolites, the intestinal epithelial cells express not only PRRs but can recognize microbial metabolites as well. Examples include secondary bile acids, vitamins (such as folate), indoles and short chain fatty acids (SCFA) – propionate, butylate and acetate. The latter example is probably studied in

most detail, showing that through binding to receptors present on enteroendocrine cells the SCFA stimulate production of hormones involved in glucose metabolism and food intake. In the same time, propionate has also an immuno-regulatory function by stimulating production of anti-microbial factors. (Cani, 2018) The interconnection of immune system with metabolic functions is even better depicted by the effects of pathogen recognition by the immune cells. Certain PAMPs, such as bacterial lipopolysaccharide (LPS), have been observed to cause inflammation and insulin resistance, causing changes in hosts metabolism. These alterations are associated with obesity and diabetes. (Cani, 2018)

In many cases, studies performed on individuals with metabolic disorders show different microbiota profiles compared to healthy individuals. The character of these associations is not clear (causational or consequence). For instance, a study by Mar Rodriguez et. al (2015) performed on a group of obese individuals and healthy controls found a negative association between fungal genus *Mucor* and *Penicillium* and factors such as body mass index (BMI) or fat mass. The relative abundance of *Mucor* spp. was associated with weight loss as well. Conversely, a positive association was found between *Aspergillus* and adiposity. (Mar Rodriguez et al., 2015)

1.2 Gut microbiota in IBD and IBS

1.2.1 Dysbiosis

The multiple functions performed by the gut microbiota described above, as well as its connection to the brain, showcase the importance of homeostasis in the microbial community. In the same time, the balance between the commensal and the pathogenic microbes is fragile in that it is maintained by a number of different factors. Any disturbances in this balance can lead to a state of dysbiosis and promote disease.

By definition, dysbiosis is “a decrease in gut microbial diversity owing to a shift in the balance between commensal and potentially pathogenic microorganisms”. (Ni et al., 2017) However, when considering inter-individual deviations of taxonomic composition of the microbiota, it is important to note that independently of the taxonomic composition, any dysfunctional microbiota can be considered dysbiotic. Dysbiosis can be induced by certain environmental factors such as diet, drugs (antibiotics), pathogens and toxins. (Carding et al., 2015) Even though ingestion and direct contact with the irritant is the most obvious pathogenesis, because of the existence of the gut-brain-axis, external factors can also disturb the balance in the microbiota composition. Stress, both physical and psychological, and especially chronic exposure to stress is a major factor modulating microbiota composition by

promoting development of pathogenic species. (Konturek et al., 2011) The factors shaping the microbiota early in life, such as mode of delivery and diet (breast milk vs. formula) can also contribute to microbial imbalance later in life, when failing to establish a stable functioning microbial community. Finally, host genetics is believed to play a role as well. (Rodriguez et al., 2015) Evidently then, occurrence of dysbiosis is a product of multiple factors, both external and internal.

1.2.2 Inflammatory bowel disease (IBD)

IBD is a collective term for chronic immune-mediated intestinal inflammation of a complex pathogenesis, usually manifesting itself in form of Crohn's disease (CD) and ulcerative colitis (UC). (Ni et al., 2017) Symptoms include abdominal pain, diarrhea, rectal bleeding, and weight loss. CD and UC are different in terms of location and type of inflammatory changes, however because of similarities in manifestation of the disease, they are often hard to distinguish in differential diagnosis. (Fakhoury et al., 2014) Although the complete etiology of IBD is unknown, it is generally accepted that both dysbiosis and inappropriate host immune response to the gut microbiota are key factors. (Carding et al., 2015) The character of microbiota association with the disease, whether it is causational or merely correlational, is yet to be established.

The bacterial microbiota composition in IBD patients has been extensively studied and documented, and some specific microbiota trends have been identified. Fecal samples from IBD patients often show a general decrease in abundance and functional microbial diversity. A reduced proportional abundance of the Firmicutes phylum, and an increase in Bacteroidetes, as well as facultative anaerobic Enterobacteriaceae is commonly found. (Carding et al., 2015) It has been observed that the microbiota of CD and UC patients exhibit different patterns specific to the disease. A study by Sokol et. al. has shown a specific for CD reduction in *F. prausnitzii*, a bacterium thought to have an anti-inflammatory effect. (Sokol et al., 2017) Conversely, adherent-invasive *Escherichia coli* (AIEC) has been investigated because of the bacteria's ability to replicate in the epithelium. Consequently, an association between AIEC and ileal mucosa of CD patients have been observed. (Darfeuille-Michaud et al., 1998) In a similar way, certain species such as *Akkermansia muciniphila* have been negatively associated with the onset and flare of UC (Shen et al., 2018), while others, such as *Fusobacterium nucleatum* are positively associated with the development of the disease. (Ni et al., 2017)

1.2.3 Irritable bowel syndrome (IBS)

IBS is a functional bowel disorder affecting an estimated 12% of people worldwide, and is characterized by a number of gastrointestinal symptoms, as well as dysbiosis. The common symptoms, according to Rome IV criteria include abdominal bloating and distension, as well as recurrent abdominal pain (visceral hypersensitivity) associated with altered bowel habits, which can include diarrhea, constipation, or a combination of both. (Lacy and Patel, 2017) On the basis of different symptomatic manifestations of the disease, IBS is classified in three main subtypes: IBS-C (IBS with predominant constipation), IBS-D (IBS with predominant diarrhea), and IBS-M (IBS with predominant mixed bowel habits – mixed D/C). A definite etiology of IBS has not been established because of variations in the disease presentation across patients. However, a number of risk factors involved in the pathophysiology and exacerbation of symptoms have been named. Genetics, environmental factors and psychosocial factors are thought to play a role in the disease development. The onset of symptoms is often associated with food intolerances, chronic stress, history of gastroenteritis, and diverticulitis. (Mearin et al., 2016)

Similar to IBD, specific microbiota patterns have been observed in IBS patients, clearly distinguishing between healthy and sick individuals. Culture-based studies have shown a general decrease in Bifidobacteria and Lactobacilli, and an increase in streptococci and *E. coli*, as well as *Clostridium* species. More recent studies applying molecular techniques in microbiota identification show that although IBS-associated microbiota forms a distinct cluster different from healthy individuals, there are also many inconsistencies within the group. (Simrén et al., 2013) Arguably, this is due to both different etiologies and manifestations of IBS across individuals.

1.2.4 Mycobiota in IBD and IBS

In the recent years, mycobiota has earned an increased interest in studies of IBD and IBS. Already in 1990, the role of fungi in pathogenesis of CD has been noted. A study by McKenzie (1990) has drawn the attention to the presence of anti-*Saccharomyces cerevisiae* antibodies (ASCA) in CD patients. In this study a serological test has been performed on IBD patients, including both CD and UC patients, as well as healthy controls. A presence of IgG serum antibodies against 11 out of 12 strains of *S.cerevisiae* was detected, as well as against two major serotypes of *C.albicans*. (McKenzie et al., 1990) Since then, an association between fungi and IBD has been established. A later study by Standaert-Vitse (2006) has identified *C. albicans* as an immunogen for ASCA, causing the inappropriate immune response in CD patients. (Standaert-Vitse et al., 2006) Findings like these rise the question of

fungal composition in the gut, and whether a presence or overrepresentation of certain species can be involved in the disease onset. A number of more recent studies aimed to identify the mycobiota of IBD patients, particularly CD patients. A study by Lewis (2015) reported an increased abundance of fungi, strongly associated with bacterial dysbiosis in pediatric CD patients compared to healthy controls, although the same fungal taxa were present in both groups. (Lewis et al., 2015)

Probably the most comprehensive study to date was performed by Sokol, in which study the fungal and bacterial composition of the faecal microbiota was determined in 235 IBD patients. Significant alterations in the mycobiota of IBD patients were observed compared to healthy controls. The authors named *Saccharomyces*, *Debaromyces*, *Penicillium*, *Kluyveromyces* and *Candida* as the most dominant genera. The study reported increased Basidiomycota/Ascomycota ratio, as well as increased abundance of *C. albicans* and decreased *S. cerevisiae*. Moreover, whereas bacterial biodiversity was decreased in all IBD patients, the decrease in fungal biodiversity was only observed in UC patients, suggesting overgrowth of fungi on the expense of bacteria in CD-specific gut environment. (Sokol et al., 2017) These results are somewhat confirmed by other studies by Liguori (2015) and Li (2014), reporting similar changes in mucosa-associated microbiota of CD patients. (Liguori et al., 2016) (Li et al., 2014b) It is then fairly clear that certain associations can be found between fungal microbiota and IBD.

The mycobiota of IBS patients is much less studied, even though a few studies attempted to characterize the composition and establish possible associations between fungi and the disease. One study by Botschuijver performed on IBS patients as well as rats exhibiting visceral hypersensitivity showed a strong association between fungal patterns and the experienced visceral hypersensitivity. The fungal profile of the IBS patients differed significantly from that of healthy controls. In addition, administration of a fungicidal in rats resulted in reversal of visceral hypersensitivity to normal sensitivity level. (Botschuijver et al., 2017) However, more detailed studies are needed, as specific fungal species could play a role in the inflammatory mechanisms. For instance, the role of *C. albicans* as a possible cause of the symptoms experienced by IBS patients has been proposed (Santelmann and McLaren Howard, 2005), while *Saccharomyces boulardii* has been observed to reduce gastrointestinal dysfunction and inflammatory reaction in rat IBS models. (Brun et al., 2017)

1.3 Gut microbiota diagnostics

Gut microbiota diagnostics is a wide field of study in research, but a relatively unknown ground in clinical practice. In diagnostic context, the focus has rather been on identifying pathogens than taking a holistic approach. Gut microbiota diagnostics have for a long time been reliant on culture-based methods, such as growth on selective media, biochemical assays and microscopy. The development of molecular techniques opened new possibilities for more accurate and time-effective detection of microbial communities. Sequencing-based methods allow identification of microbial taxa present by targeting specific gene regions, and when connected with use of complex databases, provides the best representation of the communities present in the sample. However, these methods are unlikely to be introduced in contemporary diagnostics, as they impose high costs connected with sample preparation and reagent use.

1.3.1 Sequencing-based methods

Next generation sequencing (NGS) collectively describes sequencing methods developed by different companies to enable faster and more efficient sequencing. The term includes 454 pyrosequencing, ion torrent semiconductor sequencing, sequencing by ligation (SOLiD) and reversible terminator sequencing (Illumina sequencing). In a typical workflow for Illumina sequencing, the DNA is first extracted from the sample, followed by amplification of the target genes and library preparation for sequencing. The choice of primers for template generation is an important step, as it determines the efficiency of correct OTU identification. For bacterial identification, 16S rRNA gene makes an ideal target, due to it containing highly conserved regions identical for all bacteria, as well as hypervariable regions which allow for determination of genetic distance and thus enables taxonomical identification as narrow as species level. (Janda and Abbott, 2007)

For fungal identification, the ribosomal DNA operon has been mostly recommended as a target for these primers, including 26S, 5.8S, 18S and ITS regions. The 18S region has been widely used in studies of mycobiota, as a parallel to bacterial 16S rRNA gene. However, in contrary to 16S gene, which over the course of evolution has developed many variable regions, 18S is much less diverse and lacks variation in closely related fungal species. Conversely, the ITS region includes both highly conserved sequences as well as variable sequences (both in length and sequence similarity), making it possible to distinguish between different fungi on species level. Therefore, the use of primers targeting the ITS region is commonly considered the “gold standard” for identification of fungi. (Huseyin et al., 2017) Choice of only one primer pair has been challenged by Tedersoo and Lindahl, who in their study from 2016 outlined how minor mismatches to target sequences of the primers ITS1F

and ITS2 can discriminate clinically relevant fungal taxa. Based on these findings, the authors recommend a use of primers covering both ITS and 18S (as well as 28S) rDNA regions for fungi analysis. (Tedersoo and Lindahl, 2016)

1.3.2 GA-map® Dysbiosis Test

GA-map® Dysbiosis Test is a clinically validated, probe based solid phase assay designed to identify specific bacteria present in the sample and rate the dysbiosis level in accordance with the microbiota profile of the sample. The classification of microbiota profiles is based on results of diverse microbiota studies which enabled establishment of a normobiosis microbiota profile, and identification of specific bacteria on different taxonomical levels associated with disease. The test includes use of fifty-four probes targeting variable regions of the bacterial 16S rRNA gene (V3-V7) for identification of bacteria present in the sample. Quantitative deviations from normobiosis are measured and algorithmically assessed to result in a Dysbiosis Index (DI) scored from 1-5, where 5 is severe dysbiosis. GA-map® Dysbiosis Test performed on a group of IBD and IBS patients, as well as healthy controls, showed a significantly different distribution of DI between IBD, IBS patients and healthy individuals. (Casen et al., 2015)

GA-map® Dysbiosis Test shows a potential as a diagnostic tool in IBD and IBS. The current tools most commonly used in IBD diagnosis include colonoscopy, X-ray computed tomography and magnetic resonance imaging scans, biopsies with histologic and cytologic examinations, as well as laboratory blood tests (total blood count, B12 levels). (Fakhoury et al., 2014) The diagnosis of IBS is empirical, following the Rome IV criteria, and is often based on exclusion of other diseases (celiac disease, IBD). (Simrén et al., 2013) The symptoms of both IBD and IBS often resemble each other, but there is no biochemical explanation for the symptoms in IBS. While many of the IBD diagnostic tools are invasive and non-cost-effective, some tests, such as fecal calprotectin, have been proposed to distinguish between the diseases. (Walsham and Sherwood, 2016) GA-map® Dysbiosis Test presents a new approach that aims to include the assessment of dysbiosis in diagnosis of IBD and IBS as well as a follow-up of the treatment. It is a highly reproducible, high throughput multiplex assay, giving rapid results of high accordance with sequencing-based methods. (Casen et al., 2015) Including microbiota profiling in the diagnosis and treatment processes gives potential prospects of more accurate diagnosis and more effective treatment, for example by using microbiota as a target of treatment.

1.3.3 LAD – Liquid Array Diagnostics

An increased demand for microbiota profiling in clinical context creates a need for efficient high throughput tools that can be used in diagnostics at a relatively low cost. The GA-map, although it fills the void for clinically applicable microbiota profiling tools, is relatively expensive due to the solid-phase hybridization it relies on. Therefore, a new method liquid array diagnostics (LAD) has been developed. As an improvement to GA-map, LAD enables rapid detection of up to 50 biomarkers in a single tube multiplex reaction, based on liquid-phase hybridization. (Hiseni et al., 2019) LAD is performed in three steps: labelling reaction, reporter probe (RP) addition and melting curve analysis (all steps are presented in Figure 1). The method is based on duplex formation from two types of probes: one labelled with a quencher molecule if the target DNA is present, while the other carries a fluorophore. In the presence of target DNA, the fluorescence is therefore quenched. Use of different channels of detection combined with specific melting profiles of the duplexes enables detection of multiple targets in a single reaction. (Hiseni et al., 2019)

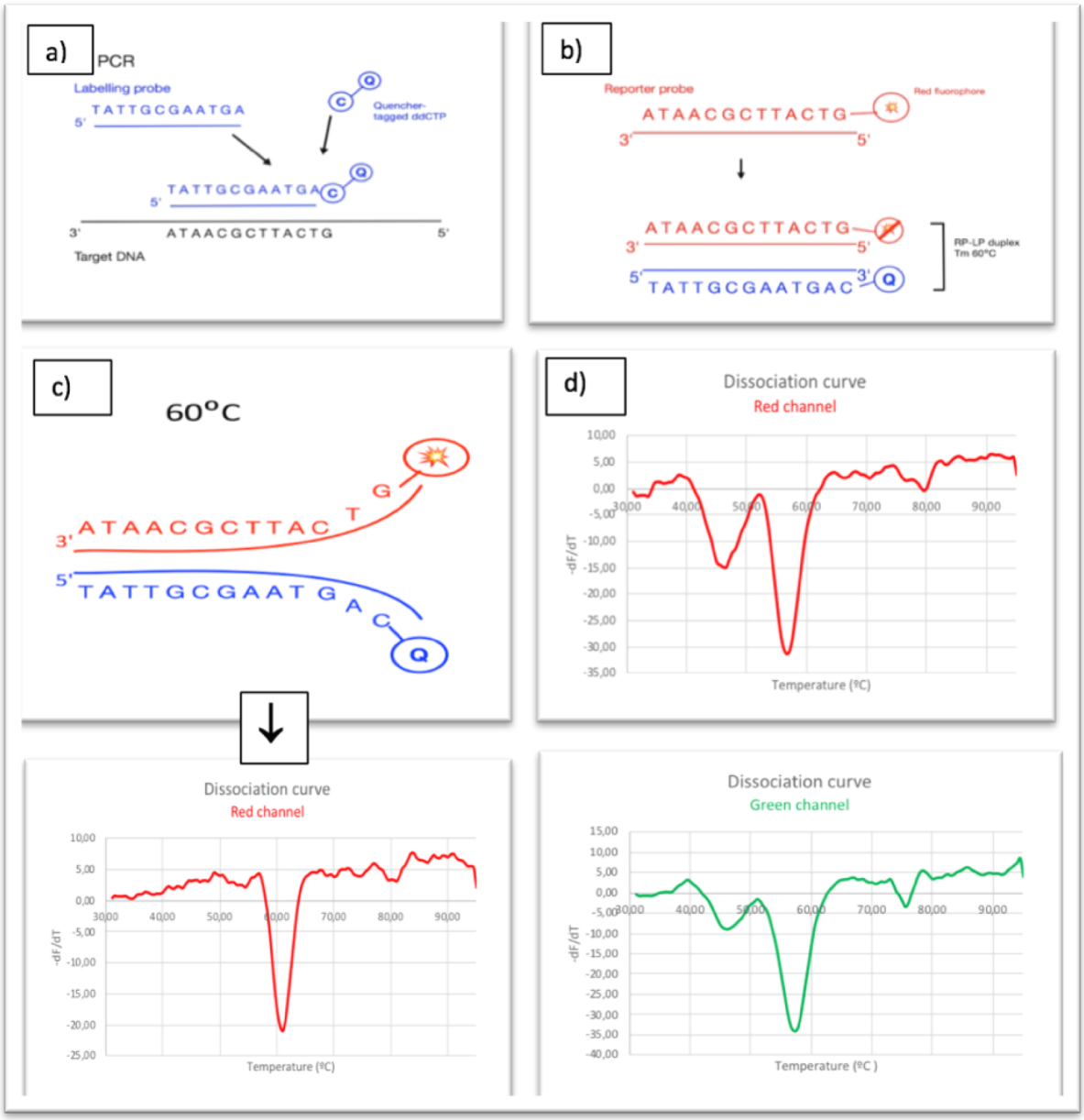

Figure 1. Liquid Array Diagnostics. *a) Labelling probes (LP) and quencher-tagged ddCTPs are added to a PCR with the target DNA. The LPs are short sequences complementary to the template DNA, with their 3' end always opposite to a G. If the target DNA is present, the probe will get elongated by one nucleotide only – the quencher-tagged ddCTP – and thereby labelled. b) Addition of RPs results in formation of LP-RP duplexes. The fluorophore attached to RPs 5' end comes in proximity with the quencher of the LP, causing a drop in fluorescence emission. c) The melting curve analysis reveals which targets are present in the sample. Each LP-RP duplex has a specific melting temperature, at which temperature a signal will be observed. d) Using different channels for fluorescence detection allows for detection of multiple duplexes with different melting temperatures.*

1.4 Aim of the study

Growing evidence that fungi are important actors in human health and disease rise the question of inclusion of fungal species in gut microbiota profiling tools. As outline in the case of IBD and IBS, fungi have been associated with dysbiosis, especially in CD patients. Inclusion of probes targeting fungi in LAD could improve the method for diagnostic use, helping to distinguish between CD and other forms of IBD as well as IBS.
LAD has been successfully used to detect bacterial species, targeting their 16S rRNA gene. (Hiseni et al., 2019) Using the same principle of probe-based detection, sequences of 18S rDNA or ITS region could be potential targets facilitating the detection of clinically relevant fungi.

The main aim of this study was to assess fungi as potential probe targets in LAD, and to see how LAD signals produced by fungi correspond with DI scores produced by GA-map®. To achieve that, additional goals were set as follows:

- To quantify eukaryotic and fungal DNA, as well as bacterial DNA in fecal samples of patients with dysbiosis.
- To establish a ratio of fungal to bacterial DNA in these samples.
- To identify the fungal taxa present in the samples by Illumina sequencing and compare their composition with results of other studies of IBD and IBS patients.
- To choose relevant fungi as targets for probe design.

2. Materials and methods

This study was a part of a bigger project aiming to develop LAD as a supplementary method for the existing GA-map® Dysbiosis Test. Previous experiments included bacterial probes only, yet some recent studies outlined the presence of fungi (Schei et al., 2017) and their potential role in dysbiosis. (Sokol et al., 2017) The potential of LAD probes targeting fungi was explored in this study, following a workflow which is presented below (figure 2).

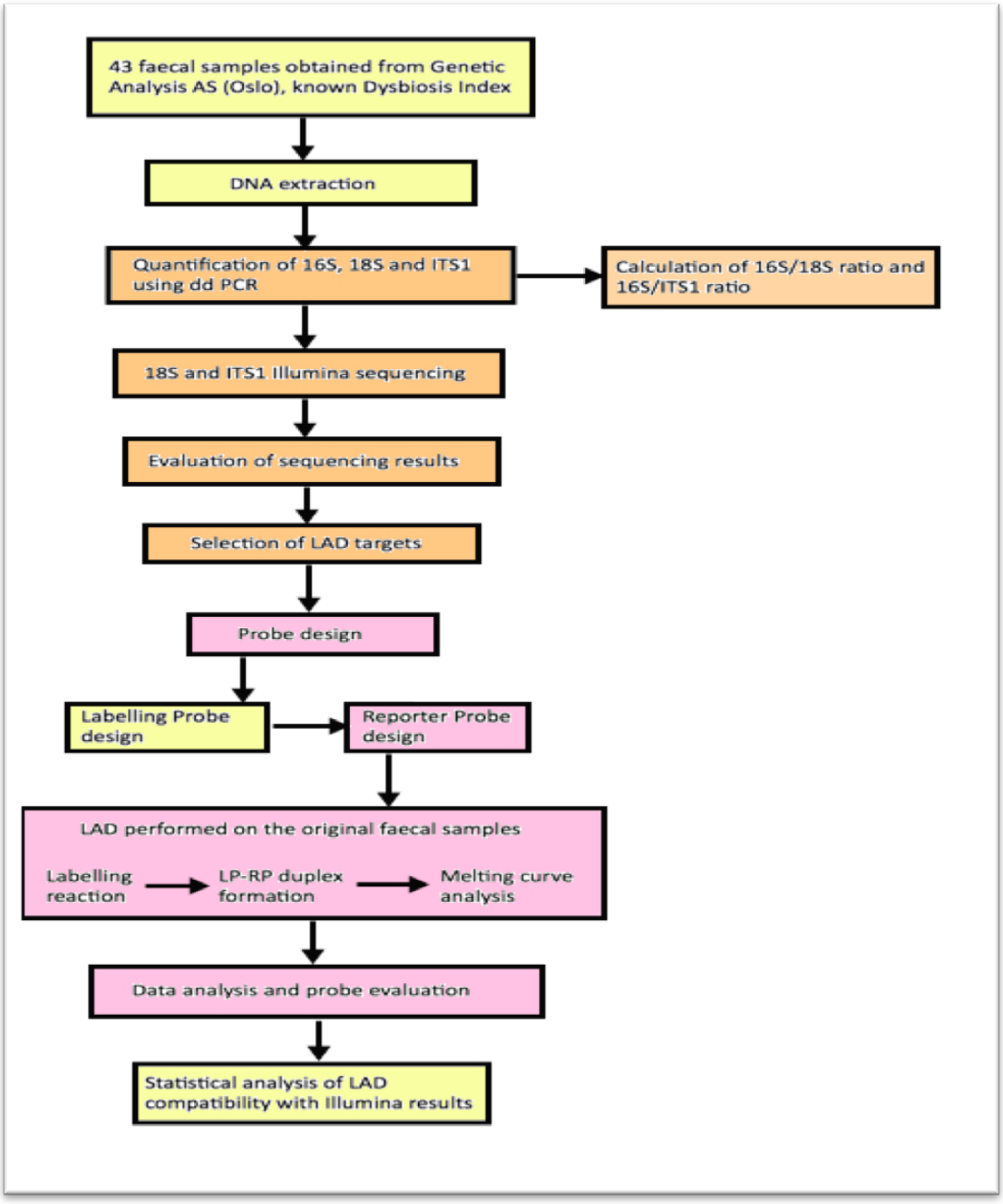

Figure 2. Flow chart of the study. *The sample preparation steps and the steps marked in yellow were performed by Pranvera Hiseni (Genetic Analysis AS). During the course of this project the workflow was divided into data generation, including sequencing (in orange) and LAD experiment (in pink).*

2.1 Faecal samples

43 faecal samples with a known DI (GA-map® Dysbiosis Test) were obtained from Genetic Analysis AS (Oslo, Norway). The dataset analysed in this study thus comprised of samples with DI from 2-5. The distribution of the DI scores was as follows: DI 2: n=2, DI 3: n=11, DI 4: n=17 and DI 5: n=13. The samples were frozen and thawed in room temperature.

2.2 DNA extraction

The DNA extraction was performed using GA's standard protocol for DNA extraction. The DNA was extracted directly from the faecal samples using FastPrep® lysing matrix E. Matrix E is the standard lysing matrix used at GA for DNA extraction from faecal samples. FastPrep® lysing matrix E is composed of 1,4mm ceramic spheres, 0,1mm silica spheres, and 4mm glass beads. (MP Biomedicals)

2.3 Quantification by ddPCR

Droplet digital PCR (ddPCR) was performed on the extracted gDNA to obtain absolute quantification of bacterial and fungal DNA present in the samples. The principle of ddPCR is based on water-oil emulsion technology, where droplets containing the template are formed and allow for independent amplification of the target in each droplet. The final concentration of the template is determined by fluorescent signal emitted by template-positive droplets and calculated by applied statistical analysis. (Hindson et al., 2011)

16S rRNA gene was the target for quantification of bacterial DNA, while 18S rRNA and ITS1 region of eukaryotic DNA were used to quantify the fungal DNA. The purpose of the quantification was to calculate the bacteria to fungi ratio in the samples. The samples were prepared by diluting in nuclease free water 1:1000 and 1:10 for 16S analysis and both eukaryotic analyses respectively. The dilutions were chosen according to the results of a test measurement which featured a dilution series. The reaction mix was prepared by adding 2,3µl template DNA to 11,5µl 2x QX 200™ EvaGreen ddPCR™ Supermix (Bio-Rad Laboratories), 8,28µl nuclease free water, 5µl forward primer and 5µl reverse primer. The primers used in each reaction are listed in Table 1. 20µl reaction cocktail was put in a cartridge together with 70µl Droplet Generation Oil for EvaGreen® (Bio-Rad) for each sample and the droplets were generated using QX 200™ Droplet Generator (Bio-Rad).

Table 1. Primers used in ddPCR reactions.

Reaction	Forward primer	Primer sequence 5'-3'	Reverse primer	Primer sequence 5'-3'
16S	341F	CCTACGGGRBGCASCAG	806R	GGACTACYVGGGTATCTAAT
18S	3NDF	GGCAAGTCTGGTGCCAG	V4_EVK	ACGGTATCTRATCRTCTTCG
ITS1	BITS	ACCTGCGGARGGATCA	B58S3	GAGATCCRTTGYTRAAAGTT

2.4 Preparing the library for Illumina sequencing

Illumina sequencing requires a number of preparation steps to ensure a successful analysis. The steps include template generation by PCR amplification of the target gene, adapter ligation for correct identification of the samples during sequencing, normalization and pooling of the library for an even read distribution, and library quantification.

2.4.1 Amplification of the target gene sequences by PCR

Amplification of the target sequences was performed using the primers listed in Table 1. All primers used in PCR had the concentration of 10µM. The amplification of 18S was performed on 1:1 extracted genomic DNA, with 5µl template from each sample added to reaction mix with the following proportions: 5µl 5xHOT FIREPol blend master mix (Solis BioDyne), 0,5µl forward primer, 0,5µl reverse primer and 14µl nuclease-free water. Salmon gDNA was used as a positive control. The programme used on the Applied Biosystems 2720 Thermal Cycler (Thermo Fisher Scientific, USA) included initialisation at 95°C for 15 minutes followed by 35 cycles of denaturation at 95°C for 30 seconds, annealing at 59°C for 30 seconds and elongation at 72°C for 45 seconds. A final elongation step was performed at 72°C for 7 minutes, followed by a final hold at 10°C. The same proportions were used for ITS1 amplification, and the same programme, except for annealing temperature being 55°C, and the programme ending with the final hold at 4°C.

2.4.2 Gel electrophoresis

Gel electrophoresis was performed to confirm a successful amplification of the target DNA. The products were separated by DNA fragment size on 1,5% agarose gel - a solution of UltraPure™ Agarose (Invitrogen, USA) and 1x TAE buffer. The gel was mixed with 12µl PeqGREEN DNA/RNA dye and the electrophoresis was performed in LKB Bromma 2197 Power Supply electrophoresis system on 100V for 1 hour.

2.4.3 PCR product clean-up for target sequence indexing

10µl of each of the PCR products was cleaned using the Biomek® 3000 robot (Beckman Coulter, USA), following a protocol with use of AMPure XP paramagnetic beads. This technology uses the beads' ability to bind DNA reversibly, which allows a selective clean-up of excess primers, enzymes and nucleotides. Upon addition of AMPure XP beads to the sample the amplicons bind to the beads surface. The samples are placed on a magnet and washed twice with fresh 80% ethanol. Addition of nuclease-free water separates DNA fragments from the beads, leaving the DNA resuspended in water and beads still adjacent to the magnet. While keeping the plate on the magnet, the cleaned PCR product can be easily transferred to a new plate without a need for centrifugation or filtration.

2.4.4 Index sequence addition by PCR

In this step the target DNA was amplified with addition of index sequences (adapter sequences containing a barcode sequence for sample identification in further analysis and complimentary sequences to oligonucleotides present on the sequencing flow cell). Each sample was assigned a unique combination of forward and reverse primers. The PCR was performed using 5µl of 5x FIREPol Master Mix (Solis BioDyne), 5µl of each primer, 9µl nuclease-free water and 1µl template, with the total volume per reaction being 25µl. The primers were dispensed on a PCR plate using Eppendorf epMotion 5070 robot (Eppendorf AG).

2.4.5 Normalization and pooling of the libraries

The library normalization and pooling were performed to dilute samples of higher concentrations, in order to ensure an even read distribution during the sequencing.

The DNA concentration was first measured in all samples using a standard curve of fluorescence values versus concentration. A reaction cocktail of 70µl Quant-iT™ Working Solution and 2µl sample DNA was prepared on a nunc plate. Fluorescence was measured in all samples by using Cambrex FLX800cse robot. 10 samples, ranging from highest to lowest fluorescence, were chosen from each analysis (18S diluted 1:10 in nuclease-free water) and their concentration was measured with Invitrogen™ Qubit™ fluorometer (Thermo Fisher Scientific, USA). Before measurement those samples were mixed with Quant-iT™ Working Solution in proportion 2µl sample to 98µl Quant-iT™ Working Solution. The concentrations were used to set up standard curves. Using the slope gradient and y-intercept extracted from the standard curves, the concentration values were calculated for all of the samples.

To pool the library, adequate volumes from 2-10µl were calculated for each sample based on the assumed DNA amount of 100ng for ITS1 and 60ng for 18S. The library of 18S was pooled using the Biomek® 3000 robot (Beckman Coulter), while ITS1 library was pooled by manual pipetting. The libraries were manually washed in ethanol (washed twice in 200µl 80% ethanol) while on magnet using AMPure XP beads, then removed from the magnet and resuspended in nuclease-free water. The cleaned libraries were checked on 1,5% agarose gel and quantified by laboratory personnel at MiDiv Lab (Ås, Norway) using ddPCR.

2.5 Illumina sequencing

In Illumina sequencing the target DNA is amplified in a solid phase reaction. The prepared library of adapter-ligated DNA fragments is added to a flow cell, with many oligonucleotides bound to the cell surface. DNA fragments bind to the complementary oligonucleotides and give a template for replication. The sequencing progresses in a single base manner, through addition of a single fluorophore-tagged reverse-terminator dNTP at a time. The fluorophore occupies the 3' hydroxyl position which prevents addition of the next dNTP. Before the fluorophore is cleaved away to expose the binding site for the next dNTP, the fluorescence signal is excited by laser. Hence the sequencing occurs in a real-time manner. (Buermans and den Dunnen, 2014) (Heather and Chain, 2016)

In this study, Illumina sequencing of the 18S rRNA gene and ITS1 region was performed to identify the fungal DNA and other eukaryotic DNA present in the samples and included 18S positive control (salmon DNA) and template negative control (nuclease-free water). The sequencing was performed by laboratory personnel at MiDiv Lab (Ås, Norway). Paired-read sequencing of the 18S rRNA gene and 18S rRNA gene ITS1 region were performed on a MiSeq platform (Illumina), which enables 300bp read lengths. The sequencing reads were filtered according to the quality score (minimum average q-score 25) and correct barcode matching. The further filtration of the resulting sequences was performed using UPARSE algorithm (maximal expected error was 1,0). 5000 reads per sample were used as a cut-off value to ensure that all samples were represented in like extent. ITS1 sequencing did not produce a sufficient amount of reads in any of the samples and was therefore excluded from further dataset. In the final dataset only 18S rRNA sequencing results were included, with all 43 samples and the positive control meeting the criteria, while negative control with under 5000 reads was excluded. QIIME (Quantitative Insights into Microbial Ecology) pipeline was used for quality filtering and estimation of diversity. UPARSE algorithm was used for OTU clustering, resulting in 245 OTUs. Silva rRNA

database was used for taxonomic annotation of the OTUs. Silva provides a comprehensive and updated database with focus on aligned small subunit (16S/18S) as well as large subunit (23S/28S) of rRNA sequences for both bacteria, archaea and eukarya. (Quast et al., 2013) The sequences of unidentified fungal OTUs were assigned taxonomic identity through BLAST (Basic Local Alignment Search Tool) search. (NCBI)

2.6 LAD probe design

10 most represented eukaryotic operational taxonomic units (OTUs) were chosen from 18S rRNA gene sequencing dataset for LAD probe design. 8 of these OTUs were fungal OTUs, 1 represented human DNA and one represented plant DNA. The plant DNA was not chosen for diagnostic purposes, but rather as an experiment of expansion of LAD for other purposes. This probe was therefore treated as a control probe in this study and is not discussed in depth further in this thesis. The LPs were designed using TNT Probe software tool for probe design. In order to prevent the formation of hairpin structures, heterodimers, or self-dimers, mismatches were introduced in the LP sequences. The LP sequences are listed in Table 2.

Table 2. Labelling probe sequences.

Labelling probe	**Labelling probe 5'-3' sequence**
Plants_food	CGCAGTTGTTCGTCTTTCATAAAT
Dothideomycetes	GAAGGGCATGCGG
Th_stercoreus	GCAGTAGTTAGTCTTCCGTAAAT
Pichia	CTTCTGGCTACCCCT
G_candidum	TTTAGAGTACTACCCTGAAACAT
Penicillium	CAAGAATTTCACCTCTGACAG
Microascales	CCTGTTTCCCCAGCA
Human	ACAAAATAGAACCGCGGT
D_hansenii	CAGTAGTTAGTCTTCAGGTAATC
S_cerevisiae	CAGAAGGAAAGGCCC

RPs were designed as complimentary sequences to LPs and their *T*m was adjusted using IDT OligoAnalyzer online bioinformatic tool (Integrated DNA Technologies). The RPs were fluorescently labelled at their 5' end with FAM, HEX, ROX or CY5, as described in Table 3.

Table 3. Reporter probe sequences.

Reporter probe	Fluorophore	Reporter probe sequence 5'-3'
FAM_plants	FAM	ATTTATGAAAGACGAACAACTGCG
FAM_Dothid	FAM	TTTCCGCATGCC
HEX_T_ster	HEX	ATTTACGGAAGACTAACTACTGC
HEX_Pichia	HEX	TTTAGGGGTAGCC
ROX_G_cand	ROX	ATGTTTCAGGGTAGTACTCTA
ROX_Penici	ROX	CTGTCAGAGGTGA
ROX_Microa	ROX	TTTTGCTGGGGA
CY5_Human	CY5	ACCGCGGTTCTATTTTGT
CY5_D_hans	CY5	TTTGATTACCTGAAGACTAA
CY5_S_cere	CY5	TTTGGGCCTTTCC

2.7 Detection of fungi with LAD in faecal samples

All LAD experiments were performed using amplified 18S rRNA gene using the gDNA of the original 43 samples. In the reaction cocktail, 5µl template DNA was mixed with 0,6µl forward and 0,6µl reverse primer (as specified in Table 1), 6µl 5x HOT FIREPol Blend Master Mix (Solis BioDyne) and 17,8µl nuclease-free water. Total reaction volume was 30µl. The programme used for template generation included 15-minute initialization step at 95°C, followed by 35 cycles of denaturation (30 seconds at 95°C), annealing (30 seconds at 59°C) and elongation (45 seconds at 72°C). The programme was finished with a final elongation step at 72°C for 7 minutes, and a final hold at 10°C.

2.7.1 Enzymatic clean-up of the DNA template

The PCR product was enzymatically treated with Exo I – rSAP (Thermo Fisher) – a mix of exonuclease and shrimp alkaline phosphatase - to remove excess primers and nucleotides from the samples. The Exo I - rSAP mix was calculated per 50 samples and prepared of 400µl alkaline phosphatase and 7,5µl Exonuclease. 8,15µl of the pre-mixed Exo I - rSAP solution was added to each well of the PCR plate containing 25µl of the product. The plate was then incubated at 37°C for 2 hours, followed by 15 minutes in 80°C, and cooled to 10°C.

2.7.2 Labelling reaction

For the labelling reaction, the following reaction mix was prepared: 3,5µl of 10x C Buffer, 1,4µl of 25mM magnesium chloride, 1,75µl of HOT TERMIPol® DNA Polymerase (Solis

BioDyne), 0,45µl of 40µM ddCTP-DYQ660 (DYQ660-labelled dideoxycytidine triphosphate – Jena Bioscience, Germany), 3,5µl of 10µM LP mix (comprising of equal volumes of the 10 labelling probes, as described in Table 2), 13,9µl of nuclease-free water, and 10µl of the template DNA. The final reaction volume was 35µl. Labelling reaction performed on the AB 2720 Thermal Cycler (Thermo Fisher Scientific) included 95°C initialization step for 12 minutes, followed by 30 cycles of 96°C denaturation for 20 seconds and annealing/elongation at 60°C for 40 seconds, and finished by a hold at 10°C.

2.7.3 Melting curve analysis

An RP mix was prepared consisting of 15-19,5µl RPs (10 x 10µM RPs x 1,5µl or 3 x 10µM CY5 RPs x 3µl + 7 x 10µM RPs x 1,5µl), 30µl 10% SDS and 950,5µl nuclease-free water. The final reaction mix was prepared, by adding 20µl of the RP mix to 30µl of the labelled LP mix. The melting curve analysis was performed on C1000 Touch™ Thermal Cycler (Bio-Rad), with the dissociation steps at temperatures from 31°C - 95°C, at 0,5°C intervals for 5 seconds. The dissociation curves generated by the instrument were a derivative of fluorescence and temperature (-dF/dT). A signal drop visible on dissociation curves was expected at the specific theoretic Tm of each LP-RP duplex listed in Table 4. Four dissociation curves were generated per sample, due to the use of four fluorophores (and hence four channels of detection).

Table 4. Theoretical Tm of the complimentary LP-RP duplexes.

LP-RP duplex	LP-RP duplex Tm (C°)	Channel of detection
Plants_food+FAM_Plants	60,6	FAM
Dothideomycetes+FAM_Dothid	38,9	FAM
Th_stercoreus+HEX_T_ster	58,4	HEX
Pichia+HEX_Pichia	38,8	HEX
G_candidum+ROX_G_cand	55,8	ROX
Penicillium+ROX_Penici	45,1	ROX
Microascales+ROX_Microa	35,4	ROX
Human+CY5_Human	57,3	CY5
D_hansenii+CY5_D_hans	47,3	CY5
S_cerevisiae+CY5_S_cere	38,7	CY5

2.7.4 LAD signal detection

The dissociation curves generated by the thermocycler software were examined for visual representation of signals. A satisfactory signal was characterized by its occurrence near the theoretical Tm at the desired channel only, and clearly differing from the baseline fluorescence signal, other signals and noise. In addition, because of variable signal strength, signal threshold was calculated for each probe using their fluorescence derivative values in target-negative samples at the observed melting temperature of each probe.

2.7.5 Probe validation

Sensitivity and specificity of each probe were calculated to establish the probes' ability to correctly identify true positive results (sensitivity) and true negative results (specificity). Illumina results were used as control. An empirical cut-off value (number of Illumina reads) was set for each probe, dependant on the distribution of Illumina sequence reads for the particular OTU and probe signals produced by the equivalent target in the LAD experiment. The lowest number of Illumina reads giving a signal and still giving satisfactory sensitivity and specificity was chosen as the cut off value. The cut-off values are listed in table 5 (Results).

2.8 Statistical analysis

2.8.1 Illumina

The sequencing results were evaluated for taxonomical patterns associated with the degree of dysbiosis (DI). Alpha diversity (expressed as the number of OTUs detected per sample) was described for each DI group (2-5). Kruskal-Wallis test with Dunn's multiple comparison test was performed on the OTU dataset as well. Kruskal-Wallis test is performed to establish if any of the groups' median values differ significantly from the others, while Dunn's multiple comparison test compares mean ranks of each group against each other group to establish which one (or multiple) of the groups differs from the others. The analysis aimed to establish if there were any significant differences (given as a p-value) in the number of detected OTUs in between the DI groups. All p-values larger than 0,05 were classified as not significant. The same analysis was performed on the 8 most abundant fungal OTUs, plant- and human DNA. All analyses and graph visualisation were performed using GraphPad Prism 8 (San Diego, California, USA).

2.8.2 LAD

A multinomial logistic regression model was developed to assess LAD's accuracy in predicting the DI score based on the probe signals of all 10 probes as the variables. The DI score 2 was used as the reference score (normobiosis). The model then assessed the significance of each variable (probe target) in distinguishing between normobiosis (DI 2) and each of the other DI groups. Based on the variations in signal strength produced by the probes in each sample, the model then assessed the probability of the sample falling into a certain DI score (2-5). Four template negative samples which produced no bands in gel electrophoresis were included in this model. The model was developed and applied to the results using R software environment for statistical computing and graphics.

2.8.3 Comparative analysis

An equivalent multinomial logistic regression model was applied to Illumina sequencing results to assess the accuracy of DI score prediction using this detection method. The predictive accuracy of the two methods were compared.

3. Results

3.1 16S, 18S and ITS1 ratios

The 16S r RNA gene presence was present in detectable range for quantification in 42 of the 43 samples, while 18S rRNA was quantified in 40 samples and ITS1 was quantified in 18 samples. The ddPCR quantification showed significantly higher copy numbers of 16S gene than 18S gene and ITS1 region. The log10 of the 16S/18S ratio calculated for the samples (where applicable) with a mean of 4,76 and ranged from 2,41 to 5,56. The log10 of the 16S to ITS1 ratio was on average 4,79 and ranged from 3,22 to 5,66. The quantification results are presented in Table A1 (Appendix 1). Importantly, the 18S rRNA gene was present in the samples within the detection range, which allowed for further analysis, including Illumina sequencing. Because of the low presence of ITS1 region in quantification results the sequencing of ITS1 was performed only in relevant samples, with a purpose to supplement the 18S rRNA gene sequencing data.

3.2 Illumina sequencing of 18S rRNA gene

3.2.1 Taxonomic diversity

In 18S rRNA gene sequencing 1028837 reads were produced, with a median of 24712 reads per sample and a mean of 22863 reads per sample. Fungal OTUs were detected in all of the 43 samples (1 or more reads). Altogether, 37 fungal OTUs were detected and identified, of which one OTU (*Geotrichum candidum*) was present in all samples. Human DNA was also detected in all samples. All fungal OTUs (plus human DNA) in the proportions in which they were detected in each sample are presented in figure A1 (Appendix 2).

Fungal alpha diversity described by number of OTUs detected (see Figure 3) varied from 2-14 OTUs per sample, with an average number of detected OTUs being 5,9 for DI 5, 6,9 for DI 4, 7,8 for DI 3 and 6 for DI 2. Kruskal-Wallis test with Dunn's multiple comparison test was performed on the OTU dataset to assess the differences in the observed OTU number in between the groups. The test revealed that the alpha diversity did not differ significantly in between the groups ($p>0,05$).

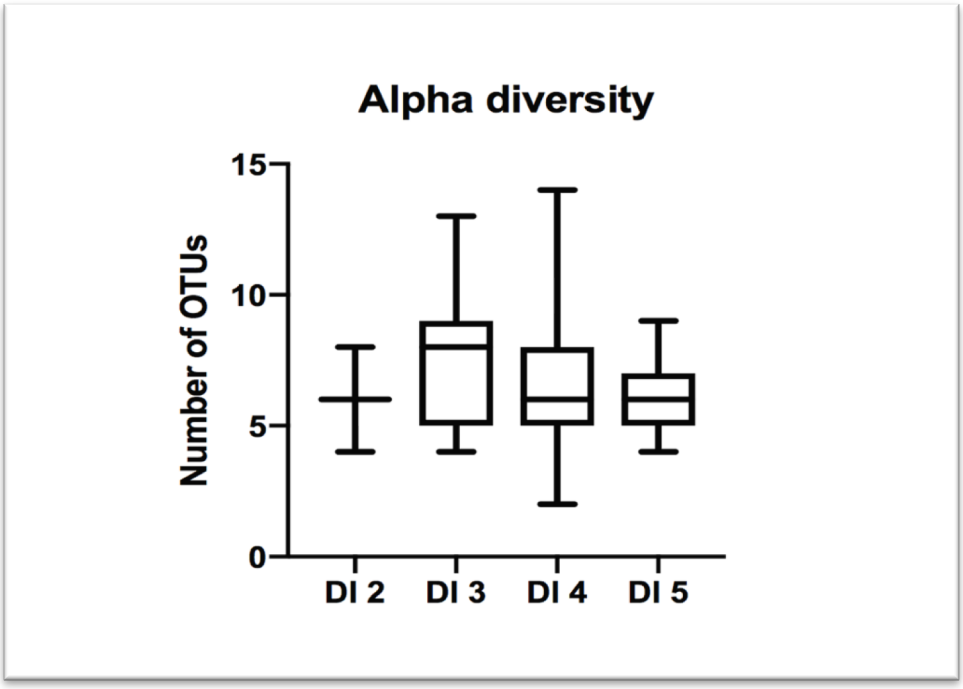

Figure 3. Alpha diversity expressed by the number of OTUs detected in each DI group. *The graph shows the median value of each group. The groups were represented in following proportions: DI 2 n=2, DI 3 n=11, DI 4 n=17 and DI 5 n=13.*

3.2.2 Taxonomic association with DI

The empirical evaluation of the sequencing data and DI of the samples did not show any clear taxonomical associations with any DI score. Kruskal-Wallis test with Dunn's multiple comparison test were performed to evaluate this observation. The test was performed on the 10 LAD probe targets. The distribution of the target OTUs in between the different DI groups is presented in figure 4. No significant differences ($p<0,05$) were found in distribution of any of the target OTUs between the DI groups.

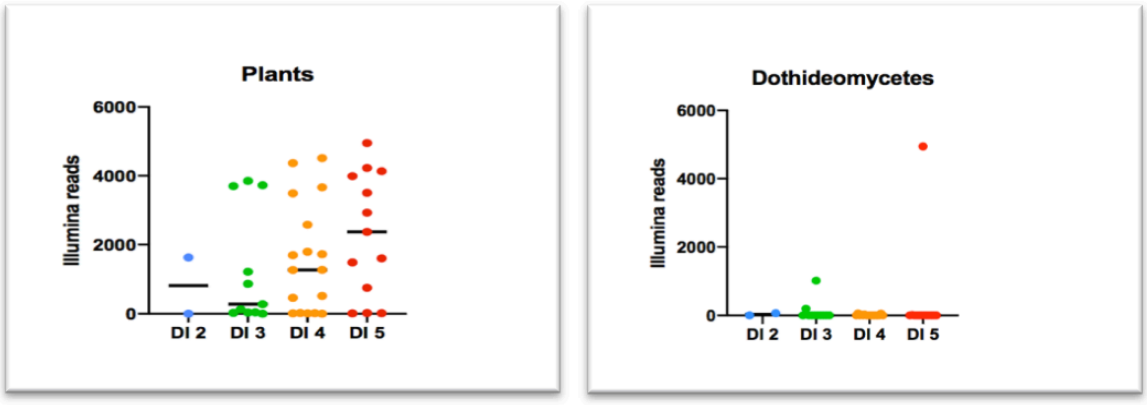

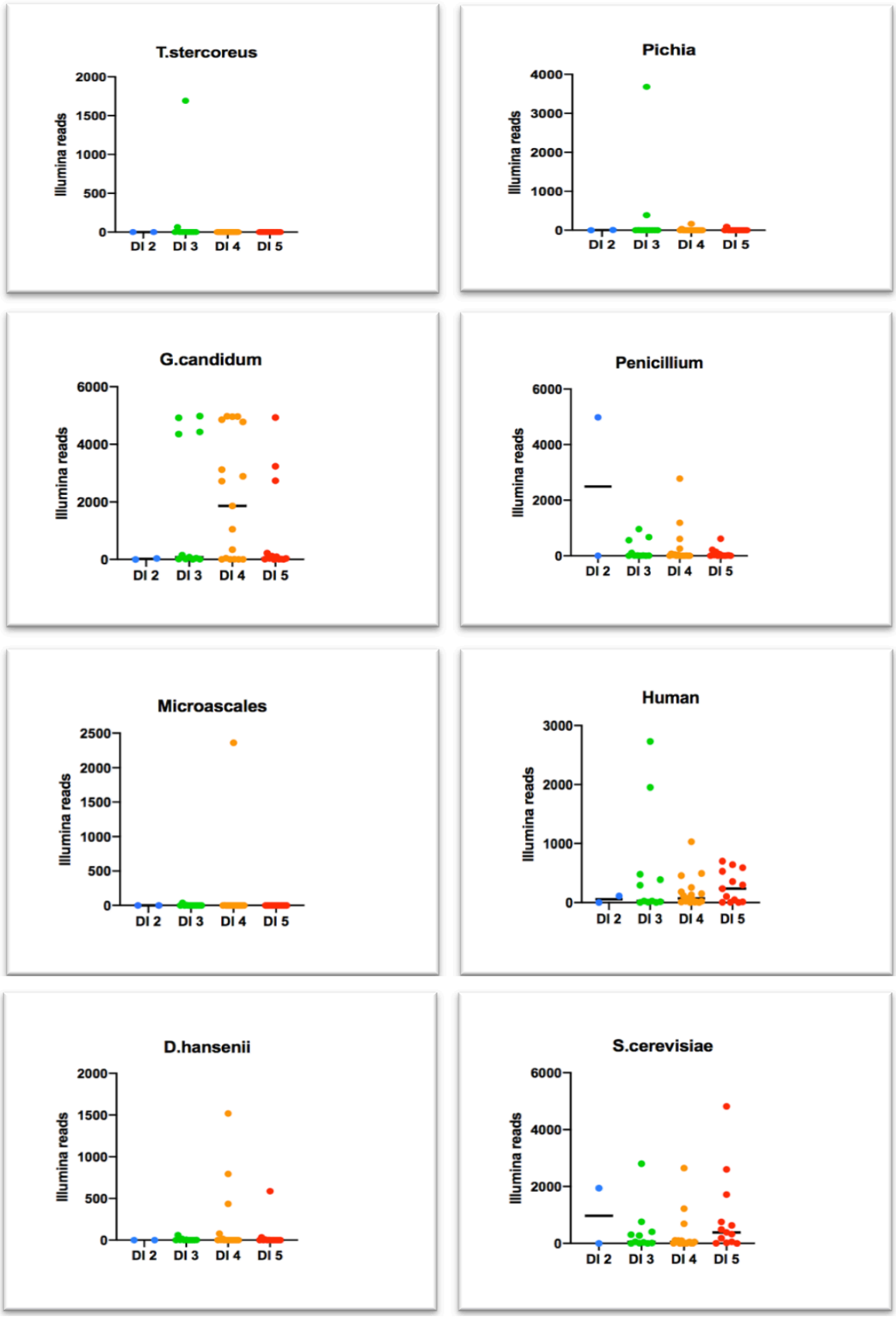

Figure 4. Distribution of the Illumina reads of the different OTUs between the DI groups. *The box plots show both the highest, the lowest and the median value in each group for each target OTU.*

3.3 Evaluation of LAD probes' performance in faecal sample diagnostics

The final LAD experiment was performed with pre-adjusted experiment conditions, including doubled CY5 RPs concentration and an additional pre-run of melting curve analysis in order to eliminate noise occurrence. In these conditions, all probes were able to produce a signal, however with variable sensitivity and specificity. Four samples were excluded from the analysis because of unsuccessful template generation (no visible bands in gel electrophoresis – see figure A2 in Appendix 3).

3.3.1 Consecutive runs of melting curve analysis on the same plate reduce noise and clarify signals

A difference in noise occurrence was observed between first and consecutive melting curve analysis performed on the same plate. The optimal results were retrieved from the second run of the same plate which was performed a day after the first analysis, after overnight incubation in room temperature. This procedure significantly reduced the noise to enable clearer observation of the produced signals. The noise was especially prevalent in the lower temperature ranges (31°C - 40°C), making it hard to distinguish between signal/no signal and producing false positive signals. In this temperature range, the problem prevailed in the consecutive runs as well. Factors such as incubation time and incubation temperature following the SDS/RP mix addition were considered as possible contributors. Incubation for 1 hour in room temperature gave no significant improvement of the dissociation curve appearance, nor did incubation in 80°C for 5 minutes followed by 1 hour in room temperature.

3.3.2 Preparation steps can influence the fluorescence levels emitted by CY5 fluorophore

An unexpected effect of SDS and/or temperature on CY5 fluorophore has been observed when combining 10% SDS with RPs and freezing the mix. CY5 fluorophore, which generally emitted lower fluorescence levels than the other fluorophores, was found to produce better results when its concentration was doubled. However, when freezing and thawing the RP mix before performing LAD, the RPs containing the CY5 fluorophore produced such low fluorescence levels that no signal could be retrieved - see figure 5. On figure 5a. (experimental setup) a few fluorescence lines starting at around 15-20 -d(RFU)/dT present 6 samples on a PCR plate where fresh RP mix was added. The clustered lines at around 5 -d(RFU)/dT show the low fluorescence emitted by samples where thawed RP mix added. No signals (peaks) can be observed in these samples. As a result of this observation, in the final

experiment setup the concentration of CY5 containing RPs was doubled, and the RP mix was prepared fresh before the RP addition step. Consequently, in this setup the fluorescence level was slightly higher, and clear peaks could be observed (figure 5b.).

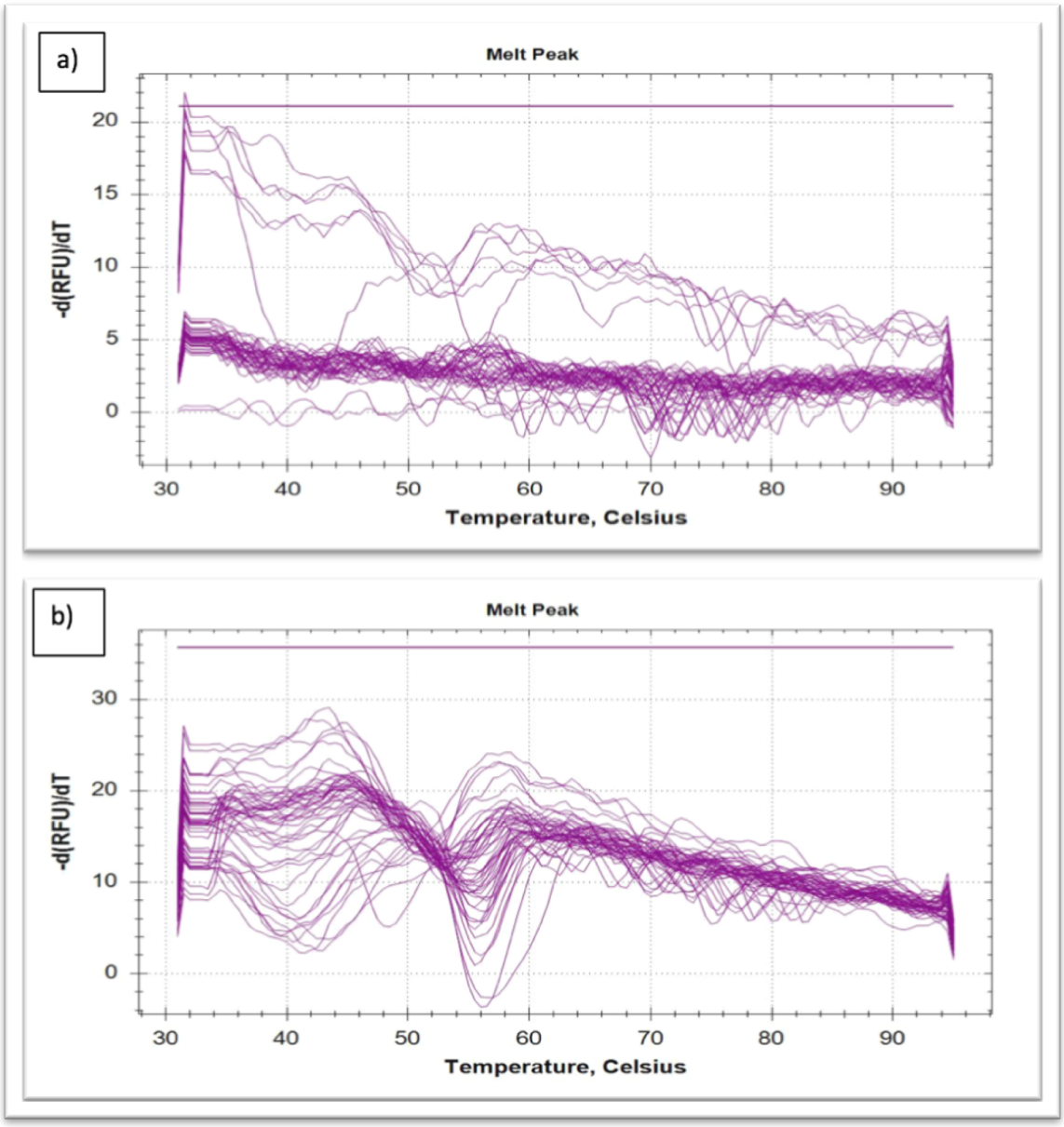

Figure 5. Differences in fluorescence emitted by CY5 fluorophore. *a.) Freezing and thawing the RP mix caused too low fluorescence emission (0-5 -d(RFU)/dT) for signals to be retrieved. 7 samples were added a freshly prepared RP mix, which resulted in visible increase in fluorescence. b.) Doubling the concentration of CY5 probes in freshly prepared RP mix caused increased and stabilised fluorescence emission.*

3.3.3 Probe signals in target-positive samples

The dissociation curves showed a good detection capability of all 10 probes. All probes were able to detect their target given that the target was represented in high copy numbers (more than 1000 Illumina reads of the target sequence). All results are presented in figure A3 (Appendix 4). Moreover, while presence of targets in big abundance resulted in very strong signals, some weaker signals were observed at lower abundances of the target. An example of this is presented in figure 6, where the same target (*G. candidum*) present in low abundance resulted in a weak signal (seen as a peak between 50°C and 60°C in the graph to the left), while in a sample where it was present in big abundance it resulted in a very strong signal (graph to the right, a peak between 50°C and 60°C). However, the correspondence of weak signals to low abundances of the target was not reliable in all of the samples. Good compliance of LAD results with Illumina sequencing results could therefore be concluded, as the strength of the signals corresponded relatively well with the abundancy of the targets reported from the Illumina sequencing results.

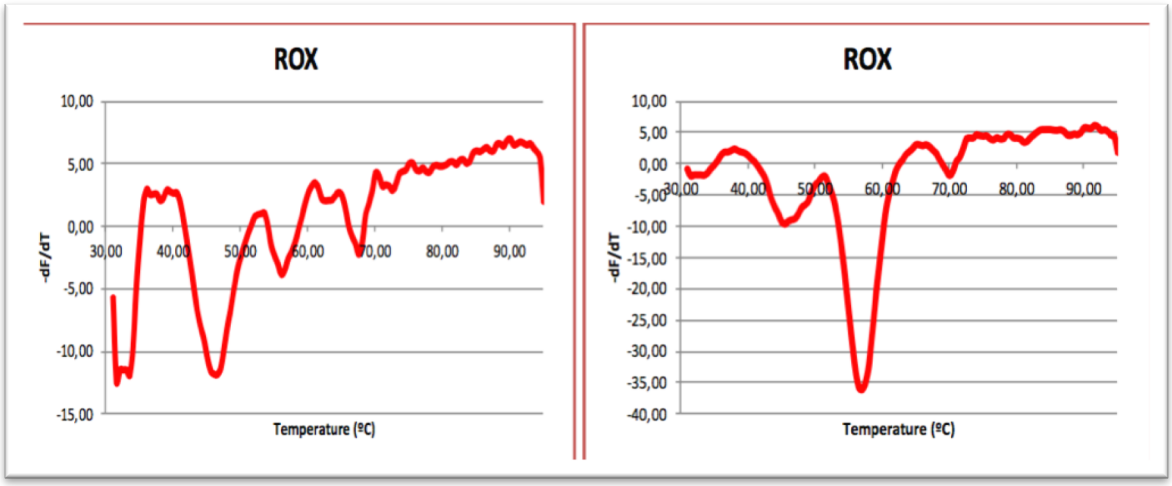

Figure 6. LAD signal strength correspondence with the abundance of the target*. A weak signal observed between 50℃ and 60℃ on the leftmost graph was an effect of lower abundance of the target G. candidum (154 Illumina reads). The rightmost graph shows a strong signal as a result of big abundance of the same target (4967 Illumina reads).*

Clearer and more defined signals were observed in temperature range from 40-60°C, while signals produced by probes with Tm under 40°C were generally less defined and hard to distinguish from noise, independently of the fluorophore used. Figure 7 shows two examples of this observation. The two upper graphs show signals produced by FAM and HEX probes at lower temperature ranges. The signals (peaks visible at around 40°C) are broad and uneven, due to some noise appearing around 31°C. In contrast to these, the two lowermost

graphs show signals produced by FAM and HEX probes at higher temperature ranges, with peaks being sharp and well defined.

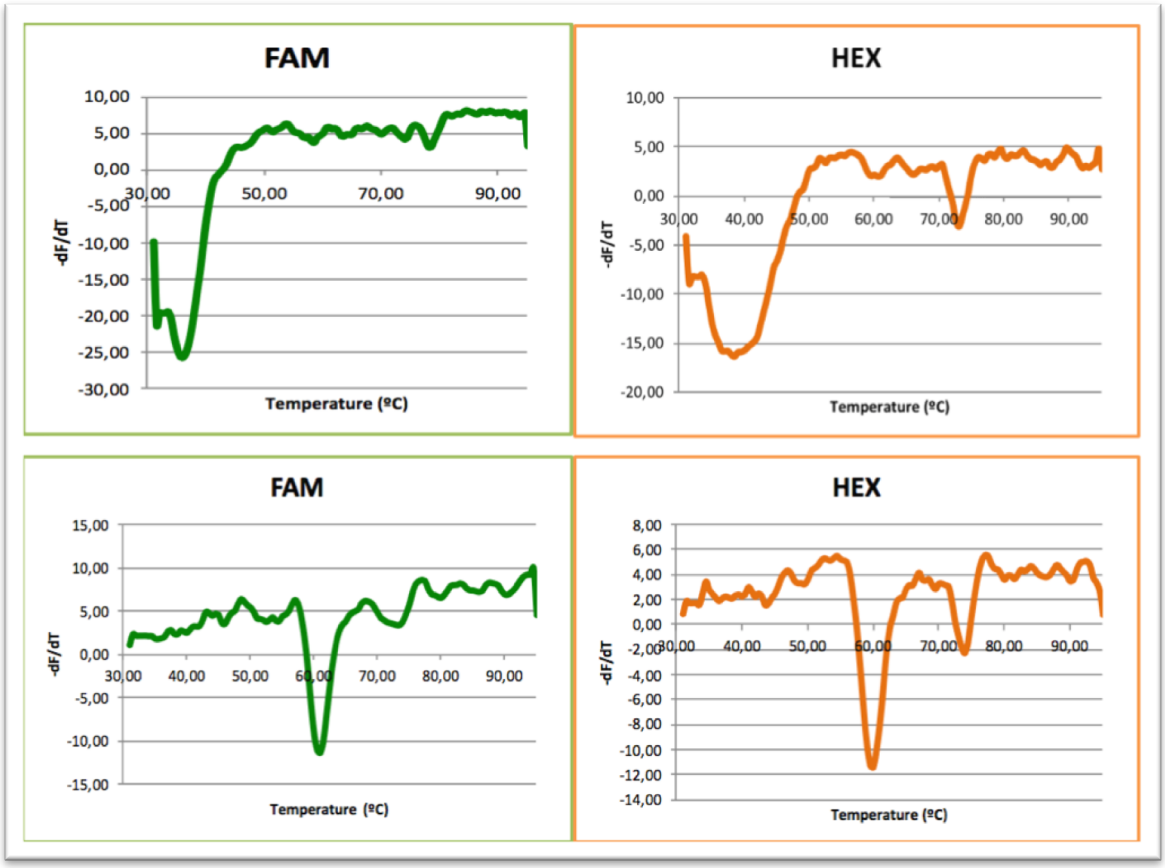

Figure 7. Signal presentation in low temperature range versus high temperature range. *Strong signals emitted by Dothideomycetes and Plants probes on FAM channel and Pichia and T_stercoreus probes on HEX channel. All signals are clearly distinguishable from baseline fluorescence signal. The signals detested in higher temperature range (under) are much more defined, while the signals present in the lower temperature range (over) are much wider and disturbed by some noise at around 31-35 ℃.*

3.3.4 Probe sensitivity and specificity

Sensitivity and specificity were calculated for each probe to evaluate its performance on mixed samples, using a cut off value based on empirical evaluation of LAD signals compared with Illumina sequencing results (table 5). Sensitivity and specificity calculated for each probe are presented in Table 6. Most probes showed good sensitivity with over 90% detection rate, except for Pichia probe and Dothideomycetes probe, which had a particularly low sensitivity. Both these probes had a low Tm (39°C). 3 probes (Pichia, G_candidum, Microascales) showed high specificity (over 90%), while 3 others (T_stercoreus, Penicillium,

Human) had a low specificity of under 70%, indicating a high rate of false positive signals produced by these probes.

Table 5. Empirical cut off values for LAD probes' sensitivity and specificity calculations.

Probe	Cut-off (Illumina reads)
Plants	275
Dothideomycetes	50
T_stercoreus	64
Pichia	166
G_candidum	154
Penicillium	60
Microascales	2361*
Human	48
D_hansenii	794
S_cerevisiae	50

*only 1 positive sample in this dataset

Table 6. Sensitivity and specificity of each probe.

PROBE	TP	TN	FP	FN	Sensitivity	Specificity
Plants	25	11	2	1	0,96	0,85
Dothideomycetes	2	26	8	3	0,4	0,76
T_stercoreus*	1	15	23*	0	1	0,39
Pichia	2	36	0	1	0,67	1
G_candidum	19	18	1	1	0,95	0,95
Penicillium*	9	15	14*	1	0,9	0,52
Microascales	1	35	3	0	1	0,92
Human	22	11	5	1	0,96	0,69
D_hansenii	2	29	8	0	1	0,78
S_cerevisiae	21	12	4	2	0,91	0,75

*off-target binding

3.3.5 False positive signals

The generally lower specificity of the probe signals can be assigned to the appearance of false positive signals throughout the analysis. In many cases no specific pattern was observed, and thereby no conclusive source of the false positive signals was found. Arguably, the false positive signals of low strength were the effect of noise occurring at lower temperature ranges and throughout the CY5 detection channel. However, 2 probes (targeting *T. stercoreus* and *Penicillium*) had a particularly low specificity attributed to the appearance of very defined false positive signals throughout the dataset. The source of these signals was investigated by empirical evaluation, in which an association of false positive signals with strong *G. candidum* signal appearance on ROX channel was observed. Off-target binding of the *T. stercoreus* and *Penicillium* probes was hypothesised and confirmed through a BLAST alignment search.

A BLAST alignment search of T_stercoreus LP sequence against *G. candidum* showed 96% identity match, with 23 out of 24 bases of the LP sequence aligning with *G. candidum* 18S rRNA gene in a complementary manner. Only a single-base mismatch was found, as shown in figure 8.

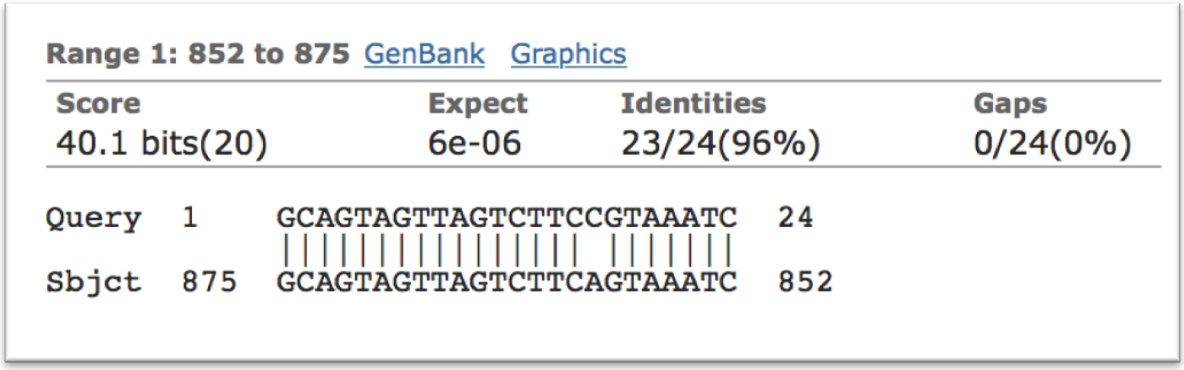

Figure 8. BLAST search result of T_stercoreus LP sequence with the quencher-tagged ddCTP at its 3' end (query 1) against G. candidum 18S r RNA gene. *The search result showed a 96% agreement with the 18S rRNA gene sequence, positions 875 to 852, including a single base mismatch at position 859.*

The BLAST alignment search of Penicillium LP sequence against *G. candidum* showed a 100% agreement of a partial sequence with *G. candidum* 18S rRNA gene, with 90% query coverage (20 of 21 bases) – see figure 9. The last LP base was not complimentary to *G. candidum* sequence, neither was the quencher-tagged ddCTP. The small extent of the mismatch would however still allow for labelling to take place.

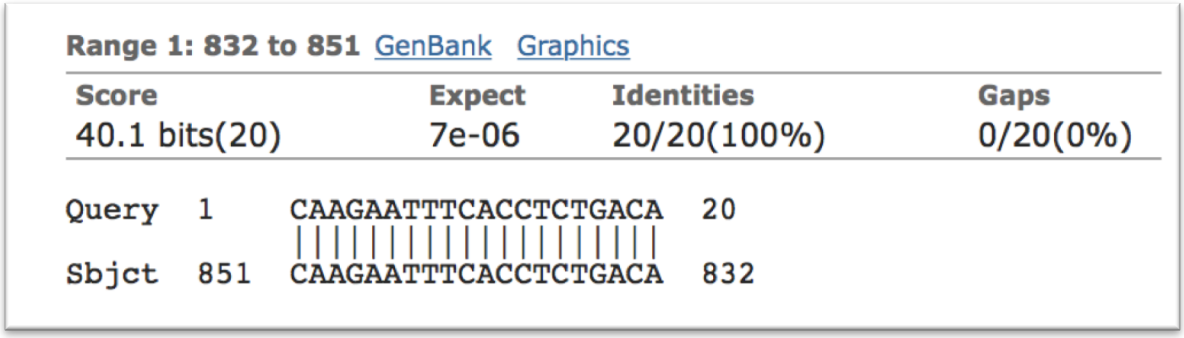

Figure 9. BLAST search result of Penicillium LP sequence against G. candidum 18S rRNA gene. *The search result showed a 100% agreement of a partial LP sequence (excluding one base and the 3' end) with G. candidum 18S rRNA gene sequence, positions 851-832. Such alignment would hypothetically still facilitate labelling, because of the mismatch being only one base.*

3.4 LAD predictive value of the samples' DI

Using a multinomial logistic regression model, LAD predictive value of DI scores was tested. As a part of the analysis, a two-tailed Z test was performed on the variables to determine the contribution of each variable to the predictive value of the model, given as a p-value, as shown in table 7. DI 2 was used as a reference, indicating that a sample falling into one of the other categories (DI 3-5) must deviate from the values detected in DI 2 samples. The table shows predictive values of each target for each DI score, providing the basis for the model. p-values lower than 0,05 were considered to have a significant contribution to the model. In this model, six of the probe targets were identified as significant variables for distinction from the reference group. These targets included *Dothideomycetes*, *Pichia*, *T. stercoreus*, *G. candidum*, *Penicillium* and *Microascales*. Using this model, 6 out of 11 samples were correctly predicted to be of DI 3, 13 out of 17 samples were correctly predicted to be of DI 4, and 9 out of 13 samples were correctly predicted to be of DI 5. The accuracy of LAD assignment of DI score to the sample (according to this model) was then calculated to be approximately 70%.

Table 7. Two-tailed Z test results from multinomial logistic regression model applied to LAD results, given as p-values.

Target	DI 3 p-value	DI 4 p-value	DI 5 p-value
Plants	0,883	0,886	0,890
Dothideomycetes	0*	0*	0*
Pichia	0*	0*	0*
T. stercoreus	0*	0*	0*
G. candidum	0*	0*	0*
Penicillium	0,005	0,003	0,001
Microascales	0*	0*	0*
Human	0,287	0,279	0,272
D. hansenii	0,267	0,267	0,272
S. cerevisiae	0,642	0,646	0,656

*the p-value is smaller than 0,05 and close to, but not equal, 0. In this case, the software presents the result as 0.

3.5 LAD compatibility with Illumina results

A corresponding multinomial logistic regression model was also applied to Illumina results. Similar to LAD results, the same targets were identified as significant contributors to the model (Table 8). Using the model, the accuracy of Illumina sequencing for prediction of DI score was calculated to be approximately 74%. 5 out of 11 samples were correctly predicted to be of DI 3, 15 out of 17 samples were correctly predicted to be of DI 4, and 10 out of 13 samples were correctly predicted to be of DI 5.

Table 8. Two-tailed Z test results from multinomial logistic regression model applied to Illumina results, given as p-values.

Target	DI 3 p-value	DI 4 p-value	DI 5 p-value
Plants	0,883	0,886	0,890
Dothideomycetes	0*	0*	0*
T. stercoreus	0*	0*	0*
Pichia	0*	0*	0*
G. candidum	0*	0*	0*
Penicillium	0,005	0,003	0,001
Microascales	0*	0*	0*
Human	0,287	0,280	0,272
D. hansenii	0,267	0,267	0,272
S. cerevisiae	0,642	0,646	0,656

*the p-value is smaller than 0,05 and close to, but not equal, 0. In this case, the software presents the result as 0.

4. Discussion

4.1 LAD probes' performance and compatibility with Illumina results

As outlined by the results, the diagnostic performance of LAD shows promise, as the assigned targets were detected by all of the probes. Moreover, although it is a theoretical model which does not consider the true diagnostic value of the probe targets, the multinomial logistic regression model used on both LAD and Illumina results shows that LAD signal reads correspond well with Illumina sequencing results.

As the aim of this study, fungi were proposed as a new target for LAD probes to complement the existing dysbiosis detection assay. The study results show that fungi can be successfully detected by LAD, although further work is needed to improve the performance of both the probes and the assay, and to adjust it for clinical use. The current probe set produced good sensitivity and specificity for the most part, while the drawbacks encountered by some of the probes provide a ground for further studies. Sensitivity and specificity of an assay are subjects to careful consideration which includes the assessment of medical consequences of potential errors. A perfect diagnostic test would be one where both sensitivity and specificity values are equal 1. This however is an unrealistic goal. Assigning a cut-off value based on either of the values (usually with help of a ROC-curve) is an adequate measure for diagnostic tests that aim to distinguish diseased individuals from healthy individuals. In some cases, when failed detection of the target would imply serious consequences for the patient, sensitivity is prioritised over sensitivity. (Habibzadeh et al., 2016) However, in case of this study and other studies of microbiota, both presence, absence and abundance of the target can contribute valuable information to the diagnosis. Improvement of both sensitivity and specificity of the probes is therefore equally important.

4.2 Diagnostic value of LAD probes used in the study

The previously mentioned studies aimed to identify the mycobiota related to gastrointestinal diseases, in particular IBD. (Sokol et al., 2017, Liguori et al., 2016, Li et al., 2014b) In these studies, certain taxonomic patterns and some potentially relevant symbiotic and pathogenic species have been identified. *Saccharomyces*, *Candida*, *Debaromyces* and *Penicillium* were mentioned among the most dominant genera. In all of these studies associations were found between *C. albicans* and inflammation, while *S. cerevisiae* was associated with healthy mycobiota. These findings make *C. albicans* and *S. cerevisiae* two of very few species that can be considered clinically relevant in IBD. However, it is important to remember that such associations say nothing about species' role in disease pathogenesis.

Identifying fungal species with a potential diagnostic value is in itself a challenging task. As pointed out in a review by Hallen-Adams and Suhr, when summing up the results of 36 studies on mycobiota, 75% of the species detected were only reported in one of these studies, while only 15 species were named in 5 or more studies. (Hallen-Adams and Suhr, 2017) One can hypothesize that many of these fungi have no clinical relevance and could have been present in the samples as a result of certain circumstances, such as its presence in the ingested food. In the same time, these numbers highlight the need of further and more extensive studies which could characterize unknown interactions of other fungal species with the gut microbiota and assess their relevance for diseases such as IBD. Although 37 fungal OTUs were detected by Illumina sequencing in this project, a vast majority of those were present in very small amounts, represented in only few samples, or were hard to identify on species level. Furthermore, the 8 fungal OTUs chosen as LAD probes targets are not necessarily clinically relevant in IBD diagnostics, but only reflect the most represented OTUs in the dataset. According to the previous studies mentioned above, a group of potentially relevant probes from this dataset would include *S. cerevisiae*, *Penicillium* and *D. hansenii*, discarding the other targets.

4.3 LAD technical performance

4.3.1 Identification of factors causing noise could improve LAD experiment outcome

Appearance of noise throughout the detection channels caused some problems with signal detection, as well as technical challenges associated with increased number of runs. Noise disturbance of the signals in lower temperature ranges affects the reliability of the probes with lower Tm, setting a challenge for detection of multiple targets through one channel. It is important to note that the appearance of these signals is not an effect of low signal strength, as is depicted by figure 5. Production of broad and uneven peaks at low temperatures is a potential error source in samples where two peaks would appear in close proximity. In this situation, an appearance of a smaller peak could be omitted in visual representation, or a false positive signal could be reported. As factors such as incubation time and temperature were excluded from causing interference, the source of the interference remains unknown. Presumably, the presence of one or more reaction components is the cause of observed differences, while incubation in the thermocycler in gradually increasing temperature during the initial run of the melting curve analysis seems to significantly reduce this effect. One potentially interfering component is the detergent SDS. SDS addition is due to its property as a DNA polymerase inhibitor (Schrader et al., 2012), which eliminates false positive

quenching upon duplex formation. In the same time, its other properties could be a cause of the observed noise. It has been observed that PCR inhibitors can interact with fluorescent probes and increase the baseline fluorescence, adding to their inhibitory properties. (Schrader et al., 2012) However, such potential action of SDS should be further investigated.

4.3.2 Polymerase infidelity is a possible cause of off-target probe binding

The choice of 18S rRNA as a detection target in LAD sets a challenge for specific probe binding. In terms of evolution, fungi have developed in relatively short period (compared to bacteria), which results in small variations of the 18S rRNA gene between closely related species. (Huseyin et al., 2017) This implies that problems can occur when distinguishing between closely related fungi and might reduce the detection to genus or family level. However, as observed in the performed LAD experiment, the cross-binding took place between seemingly unrelated species. Assuming careful design of the probes, the results rise the question of polymerase infidelity. Polymerase fidelity refers to the enzymes ability to correctly incorporate the right nucleotide over wrong ones when both correct and wrong nucleotides are present in the same proportions in a PCR. (Bertram et al., 2010) In a LAD reaction, this would mean off-target binding of probes to non-target sequences that differ with a few bases from the target sequence, which has been observed in this study.

4.4 Study limitations

Although the results presented in this study show the potential of LAD as a means of detection of pre-determined targets, the study also highlighted some biases which imposed major limitations on the diagnostic value of the fungi probes which were used.

Both Illumina sequencing results and LAD results showcase the flaws of using 18s rRNA as the target gene. Considering previous mycobiota studies which relied on sequencing, the Illumina results presented in this study lacked a comprehensive representation of the composition of the samples. The whole Basidiomycota division was absent from the experiment, while some clinically important species, such as *C. albicans*, were missed as well. *C. albicans* has been named as one of the most prevalent fungal species which inhabit the human gut and has been detected in multiple studies of the human gut mycobiome. (Hallen-Adams and Suhr, 2017) It is also one of the few fungal species that has a documented association with disease in humans. Of course, considering the limited size of the dataset, an actual absence of the species in this dataset cannot be excluded. However, the absence of *C.albicans* could also be an effect of 18s rRNA gene similarity throughout the Saccharomycetaceae family, which also includes *S. cerevisiae*, *D. hansenii* and Pichia spp.,

all present in the samples. The 18S rRNA gene is known to be a less-than-perfect target for fungi identification, since it does not always manage to distinguish between different fungi on species level. (Suhr and Hallen-Adams, 2015) Indeed, a relatively strongly represented unidentified OTUs were classified as Saccharomycetales order and Saccharomycetaceae family yet giving no further taxonomical specification. Another challenge is posed by the existing fungi databases which do not always contain the sufficient information about a fungus to identify it correctly. Consequently, some fungal OTUs can be annotated to wrong taxa, while others might simply be classified as "unclassified fungi". (Suhr and Hallen-Adams, 2015) Such challenges with fungi database annotation have been previously reported by Liguori, in whose study up to 22% of the detected fungi have been left unclassified. (Liguori et al., 2016) It could be then argued that the missing *C. albicans* is either not present in the dataset or could be "hiding" in those unidentified collective OTUs, or as an incorrectly identified member of other Saccharomycetaceae OTUs.

Another limitation is presented by the size and composition of the dataset. A relatively small set of samples (n=43) is arguably not sufficient to observe dysbiosis-related patterns. The double-blinded character of GA's research means also that information which was potentially important for this study could not be obtained. The retention of the samples, origin of the samples (multiple samples obtained from one patient) and patient diagnosis (CD, UC, IBS) could all influence the results. Furthermore, with only 2 out of 43 samples being classified as normobiosis (DI 2), the differences between dysbiotic and normobiotic samples can easily be omitted. For a statistically correct association analysis, a dataset with normobiotic and dysbiotic samples represented in comparable proportions would be recommended. Hypothetically, patterns that were not possible to extract from the present dataset would be observed in a bigger and more evenly distributed dataset.

4.5 Suggested further work

LAD has been developed as a method for dysbiosis diagnostics, which can be easily performed using standard PCR and qPCR instruments. In principle, it aims to supplement the already existing GA-map® Dysbiosis Test, simplifying the process and making it both more time- and cost-effective. Possible inclusion of fungi in the set of diagnostic probes is a new direction in the process of method development. Growing evidence from the recent research suggests that fungi play a role in dysbiosis and can potentially be used as diagnostic markers in dysbiosis associated with IBD. Based on these assumptions, the work performed in this study met a number of challenges that have to be addressed in future work.

Firstly, a thorough assessment of clinically relevant probe targets is needed. The mentioned studies provide an insight into fungal patterns which can be expected in IBD-associated dysbiosis. However, further studies are needed to establish associations with specific DI groups, or perhaps with specific diagnosis and discriminatory of other diagnoses (e.g. a pattern associated with CD diagnosis only). Moreover, just as research on bacterial dysbiosis provides a relatively reliable evidence for contribution of specific bacterial taxa to dysbiosis, IBS, and IBD, the study of mycobiota is in comparison still in its infancy. This, arguably, poses the biggest challenge for possible inclusion of fungal probes in LAD dysbiosis analysis.

Although no errors have been observed to be related to probe design, improvements are needed in respect to probe targets choice and probe validation. The 18S rRNA gene which was used as the target gene in this study is not an ideal target due to too little variation in the gene between fungal species. ITS have been named as the optimal target, allowing for identification of fungi on species level, as opposed to genus or family level with 18S rRNA. (Huseyin et al., 2017, Suhr and Hallen-Adams, 2015) In this study, although detection of fungi with ITS1 region was attempted, an unexpected pitfall was met when the DNA fragments were presumably discarded during the clean-up procedure. Redesigning the experiment setup with successful sequencing of ITS as the target DNA could bring a substantial improvement to the diagnostic value of the probes. Probe validation on pure-culture samples would further reduce the uncertainty associated with probe binding accuracy.

Finally, the technical aspects of LAD need further work and adjustments to optimize the assay's diagnostic performance. Assessment of SDS's role in noise interference and an evaluation of different polymerases to minimise off-target binding should be performed. Elimination of noise from the initial run of melting curve analysis would significantly reduce the time aspect of LAD, increasing the efficiency of the assay compared to other methods. It would also contribute to reduction of false positive and false negative signals occurrence. Off-target binding was the other identified factor causing false positive signals. The use of a high-fidelity polymerase could potentially reduce this effect and further contribute to increasing LAD sensitivity and specificity. Addressing these technical issues could also improve accuracy of the assay, as calculated for the multinomial logistic regression model, and bring it closer to the accuracy of Illumina sequencing.

4.6 Conclusion

In this study, fungi were detected in faecal samples using LAD and the correspondence of the detected targets to the degree of dysbiosis in the samples was assessed. LAD has been previously used to successfully detect certain bacterial taxa that correlate to dysbiosis. The assay is proposed to complement the currently existing GA-map® Dysbiosis Test, employing the same probe-based principle of detection, but in the same time addressing the subjects of cost-effectivity and availability in clinical laboratories. The addition of fungal probes to the assay could help improve the method in terms of further improvement of its diagnostic value. According to previous studies, the presence or absence of certain fungal species could be indicative of some medical conditions and discriminative of others, as in the case of *S. cerevisiae* and *C. albicans*. However, since no such patterns were revealed in this study, more work on this subject is needed before any technical issues, such as performance of the probes, can be addressed. More extensive studies on taxonomical patterns of the gut mycobiota in dysbiotic samples and their potential indication of medical conditions related to dysbiosis are needed. If results of previous observations can be reproduced, the fungal probes show a great potential of improving LAD's value in dysbiosis diagnostics.

Reference list

Bertram, J. G., Oertell, K., Petruska, J. & Goodman, M. F. 2010. DNA polymerase fidelity: comparing direct competition of right and wrong dNTP substrates with steady state and pre-steady state kinetics. *Biochemistry,* 49**,** 20-8.

Bonaz, B., Bazin, T. & Pelissier, S. 2018. The Vagus Nerve at the Interface of the Microbiota-Gut-Brain Axis. *Front Neurosci,* 12**,** 49.

Botschuijver, S., Roeselers, G., Levin, E., Jonkers, D. M., Welting, O., Heinsbroek, S. E. M., De Weerd, H. H., Boekhout, T., Fornai, M., Masclee, A. A., Schuren, F. H. J., De Jonge, W. J., Seppen, J. & Van Den Wijngaard, R. M. 2017. Intestinal Fungal Dysbiosis Is Associated With Visceral Hypersensitivity in Patients With Irritable Bowel Syndrome and Rats. *Gastroenterology,* 153**,** 1026-1039.

Brun, P., Scarpa, M., Marchiori, C., Sarasin, G., Caputi, V., Porzionato, A., Giron, M. C., Palu, G. & Castagliuolo, I. 2017. Saccharomyces boulardii CNCM I-745 supplementation reduces gastrointestinal dysfunction in an animal model of IBS. *PLoS One,* 12**,** e0181863.

Buermans, H. P. & Den Dunnen, J. T. 2014. Next generation sequencing technology: Advances and applications. *Biochim Biophys Acta,* 1842**,** 1932-1941.

Cani, P. D. 2018. Human gut microbiome: hopes, threats and promises. *Gut,* 67**,** 1716-1725.

Carding, S., Verbeke, K., Vipond, D. T., Corfe, B. M. & Owen, L. J. 2015. Dysbiosis of the gut microbiota in disease. *Microb Ecol Health Dis,* 26**,** 26191.

Casen, C., Vebo, H. C., Sekelja, M., Hegge, F. T., Karlsson, M. K., Ciemniejewska, E., Dzankovic, S., Froyland, C., Nestestog, R., Engstrand, L., Munkholm, P., Nielsen, O. H., Rogler, G., Simren, M., Ohman, L., Vatn, M. H. & Rudi, K. 2015. Deviations in human gut microbiota: a novel diagnostic test for determining dysbiosis in patients with IBS or IBD. *Aliment Pharmacol Ther,* 42**,** 71-83.

Darfeuille-Michaud, A., Neut, C., Barnich, N., Laderman, E., Di Martino, P., Desreumaux, P., Gambiez, L., Joly, B., Cortot, A. & Colombel, J. F. 1998. Presence of adherent Escherichia coli strains in illeal mucosa of patients with Crohn's disease. *Gastroenterology,* 115**,** 1405-1413.

Dollive, S., Peterfreund, G. L., Sherrill-Mix, S., Bittinger, K., Sinha, R., Hoffmann C., Nabel, C. S., Hill, D. A., Artis, D., Bachman, M. A., Custers-Allen, R., Grunberg, S., Wu, G. D., Lewis, J. D. & Bushman, F. D. 2012. A tool kit for quantifying eukaryotic rRNA gene sequences from human microbiome samples. *Genome biology,* 13.

Fakhoury, M., Negrulj, R., Mooranian, A. & Al-Salami, H. 2014. Inflammatory bowel disease: clinical aspects and treatments. *J Inflamm Res,* 7**,** 113-20.

Gentile, C. L. & Weir, T. L. 2018. The gut microbiota at the intersection of diet and human health. *Science,* 362**,** 776-780.

Habibzadeh, F., Habibzadeh, P. & Yadollahie, M. 2016. On determining the most appropriate test cut-off value: the case of tests with continuous results. *Biochem Med (Zagreb),* 26**,** 297-307.

Hallen-Adams, H. E. & Suhr, M. J. 2017. Fungi in the healthy human gastrointestinal tract. *Virulence,* 8**,** 352-358.

Heather, J. M. & Chain, B. 2016. The sequence of sequencers: The history of sequencing DNA. *Genomics,* 107**,** 1-8.

Hindson, B. J., Ness, K. D., Masquelier, D. A., Belgrader, P., Heredia, N. J., Makarewicz, A. J., Bright, I. J., Lucero, M. Y., Hiddessen, A. L., Legler, T. C., Kitano, T. K., Hodel, M. R., Petersen, J. F., Wyatt, P. W., Steenblock, E. R., Shah P. H., Bousse, L. J., Troup, C. B., Mellen, J. C., Wittmann, D. K., Erndt, N. G., Cauley, T. H., Koehler, R.

T., So, A. P., Dube, S., Rose K. A., Montesclaros, L., Wang, S., Stumbo, D. P., Hodges, S. P., Romine, S., Milanovich, F. P., White, H. E., Regan, J. F., Karlin-Neumann, G. A., Hindson, C. M., Saxonov, S. & Colston, B. W. 2011. High-throughput droplet digital PCR system for absolute quantitation of DNA copy number. *Anal Chem,* 83**,** 8604-10.

Hiseni, P., Wilson, R. C., Storrø, O., Johnsen, R., Øien, T. & Rudi, K. 2019. Liquid array diagnostics: a novel method for rapid detection of microbial communities in single-tube multiplex reactions. *BioTechniques,* 66**,** 143-149.

Hoffmann, C., Dollive, S., Grunberg, S., Chen, J., Li, H., Wu, G. D., Lewis, J. D. & Bushman, F. D. 2013. Archaea and fungi of the human gut microbiome: correlations with diet and bacterial residents. *PLoS One,* 8**,** e66019.

Huseyin, C. E., O'Toole, P. W., Cotter, P. D. & Scanlan, P. D. 2017. Forgotten fungi-the gut mycobiome in human health and disease. *FEMS Microbiol Rev,* 41**,** 479-511.

Janda, J. M. & Abbott, S. L. 2007. 16S rRNA gene sequencing for bacterial identification in the diagnostic laboratory: pluses, perils, and pitfalls. *J Clin Microbiol,* 45**,** 2761-4.

Kho, Z. Y. & Lal, S. K. 2018. The Human Gut Microbiome - A Potential Controller of Wellness and Disease. *Front Microbiol,* 9**,** 1835.

Konturek, P. C., Brzozowski T. & Konturek, S. J. 2011. Stress and the gut: pathophysiology, clinical consequences, diagnostic approach and treatment options. *Journal of physiology and pharmacology,* 62**,** 591-599.

Lacy, B. E. & Patel, N. K. 2017. Rome Criteria and a Diagnostic Approach to Irritable Bowel Syndrome. *J Clin Med,* 6.

Latuga, M. S., Ellis, J. C., Cotton, C. M., Goldberg, R. N., Wynn, J. L., Jackson, R. B. & Seed, P. C. 2011. Beyond bacteria: a study of the enteric microbial consortium in extremely low birth weight infants. *PLoS One,* 6**,** e27858.

Lewis, J. D., Chen, E. Z., Baldassano, R. N., Otley, A. R., Griffiths A. M., Lee, D., Bittinger, K., Bailey, A., Friedman, E. S., Hoffmann, C., Albenberg, L., Sinha, R., Compher, C., Gilroy E., Nessel, L., Grant, A., Chehoud, C., Li, H., Wu, G. D. & Bushman, F. D. 2015. Inflammation, Antibiotics, and Diet as Environmental Stressors of the Gut Microbiome in Pediatric Crohn's Disease. *Cell Host Microbe,* 18**,** 489-500.

Li, J., Jia, H., Cai, X., Zhong, H., Feng, Q., Sunagawa, S., Arumugam, M., Kultima, J. R., Prifti, E., Nielsen, T., Juncker, A. S., Manichanh, C., Chen, B., Zhang, W., Levenez, F., Wang, J., Xu, X., Xiao, L., Liang, S., Zhang, D., Zhang, Z., Chen, W., Zhao, H., Al-Aama, J. Y., Edris, S., Yang, H., Wang, J., Hansen, T., Nielsen, H. B., Brunak, S., Kristiansen, K., Guarner, F., Pedersen, O., Dore, J., Ehrlich, S. D., Bork, P., Wang, J. & MetaHIT Consortium. 2014a. An integrated catalog of reference genes in the human gut microbiome. *Nat Biotechnol,* 32**,** 834-41.

Li, Q., Wang, C., Tang, C., He, Q., Li, N. & Li, J. 2014b. Dysbiosis of gut fungal microbiota is associated with mucosal inflammation in Crohn's disease. *Clinical gastroenterology,* 48**,** 513-523.

Liguori, G., Lamas, B., Richard, M. L., Brandi, G., Da Costa, G., Hoffmann, T. W., Di Simone, M. P., Calabrese, C., Poggioli, G., Langella, P., Campieri, M. & Sokol, H. 2016. Fungal Dysbiosis in Mucosa-associated Microbiota of Crohn's Disease Patients. *J Crohns Colitis,* 10**,** 296-305.

Mar Rodriguez, M., Perez, D., Javier Chaves, F., Esteve, E., Marin-Garcia, P., Xifra, G., Vendrell, J., Jove, M., Pamplona, R., Ricart, W., Portero-Otin, M., Chacon, M. R. & Fernandez Real, J. M. 2015. Obesity changes the human gut mycobiome. *Sci Rep,* 5**,** 14600.

Mckenzie, H., Main, J., Pennington, C. R. & Parratt, D. 1990. Antibody to selected strains of Saccharomyces cerevisiae (baker's and brewer's yeast) and Candida albicans in Crohn's disease. *Gut,* 31**,** 536-538.

Mearin, F., Lacy, B. E., Chang, L., Chey, W. D., Lembo, A. J., Simren, M. & Spiller, R. 2016. Bowel Disorders. *Gastroenterology*.

Ni, J., Wu, G. D., Albenberg, L. & Tomov, V. T. 2017. Gut microbiota and IBD: causation or correlation? *Nat Rev Gastroenterol Hepatol,* 14**,** 573-584.

Quast, C., Pruesse, E., Yilmaz, P., Gerken, J., Schweer, T., Yarza, P., Peplies, J. & Glockner, F. O. 2013. The SILVA ribosomal RNA gene database project: improved data processing and web-based tools. *Nucleic Acids Res,* 41**,** D590-6.

Quintin, J., Saeed, S., Martens, J. H. A., Giamarellos-Bourboulis, E. J., Ifrim, D. C., Logie, C., Jacobs, L., Jansen, T., Kullberg, B. J., Wijmenga, C., Joosten, L. A. B., Xavier, R. J., Van Der Meer, J. W. M., Stunnenberg, H. G. & Netea, M. G. 2012. Candida albicans infection affords protection against reinfection via functional reprogramming of monocytes. *Cell Host Microbe,* 12**,** 223-32.

Rinninella, E., Raoul, P., Cintoni, M., Franceschi, F., Miggiano, G. A. D., Gasbarrini, A. & Mele, M. C. 2019. What is the Healthy Gut Microbiota Composition? A Changing Ecosystem across Age, Environment, Diet, and Diseases. *Microorganisms,* 7.

Rodriguez, J. M., Murphy, K., Stanton C., Ross, R. P., Kober, O. I., Juge, N., Avershina, E., Rudi, K., Narbad, A., Jenmalm, M. C., Marchesi, J. R. & Collado, M. C. 2015. The composition of the gut microbiota throughout life, with an emphasis on early life. *Microb Ecol Health Dis,* 26**,** 26050.

Santelmann, H. & Mclaren Howard, J. 2005. Yeast metabolic products, yeast antigens and yeasts as possible triggers for irritable bowel syndrome. *European Journal of Gastroenterology & Hepatology,* 17**,** 21-26.

Scanlan, P. D. & Marchesi, J. R. 2008. Micro-eukaryotic diversity of the human distal gut microbiota: qualitative assessment using culture-dependent and -independent analysis of faeces. *ISME J,* 2**,** 1183-93.

Schei, K., Avershina, E., Oien, T., Rudi, K., Follestad, T., Salamati, S. & Odegard, R. A. 2017. Early gut mycobiota and mother-offspring transfer. *Microbiome,* 5**,** 107.

Schrader, C., Schielke, A., Ellerbroek, L. & Johne, R. 2012. PCR inhibitors - occurrence, properties and removal. *J Appl Microbiol,* 113**,** 1014-26.

Shen, Z. H., Zhu, C. X., Quan, Y. S., Yang, Z. Y., Wu, S., Luo, W. W., Tan, B. & Wang, X. Y. 2018. Relationship between intestinal microbiota and ulcerative colitis: Mechanisms and clinical application of probiotics and fecal microbiota transplantation. *World J Gastroenterol,* 24**,** 5-14.

Simren, M., Barbara, G., Flint, H. J., Spiegel, B. M. R., Spiller, R. C., Vanner, S., Verdu, E. F., Whorwell, P. J. & Zoetendal, E. G. 2013. Intestinal microbiota in functional bowel disorders: a Rome foundation report. *Gut,* 62**,** 159-176.

Sokol, H., Leducq, V., Aschard, H., Pham, H. P., Jegou, S., Landman, C., Cohen, D., Liguori, G., Bourrier, A., Nion-Larmurier, I., Cosnes, J., Seksik, P., Langella, P., Skurnik, D., Richard, M. L. & Beaugerie, L. 2017. Fungal microbiota dysbiosis in IBD. *Gut,* 66**,** 1039-1048.

Standaert-Vitse, A., Jouault, T., Vandewalle, P., Mille, C., Seddik, M., Sendid, B., Mallet, J. M., Colombel, J. F. & Poulain, D. 2006. Candida albicans is an immunogen for anti-Saccharomyces cerevisiae antibody markers of Crohn's disease. *Gastroenterology,* 130**,** 1764-75.

Suhr, M. J. & Hallen-Adams, H. E. 2015. The human gut mycobiome: pitfalls and potentials--a mycologist's perspective. *Mycologia,* 107**,** 1057-73.

Tedersoo, L. & Lindahl, B. 2016. Fungal identification biases in microbiome projects. *Environ Microbiol Rep,* 8**,** 774-779.
Thursby, E. & Juge, N. 2017. Introduction to the human gut microbiota. *Biochem J,* 474**,** 1823-1836.
Tomkovich, S. & Jobin, C. 2016. Microbiota and host immune responses: a love-hate relationship. *Immunology,* 147**,** 1-10.
Walsham, N. E. & Sherwood R. A. 2016. Fecal calprotectin in inflammatory bowel disease. *Clin Exp Gastroenterol,* 9**,** 21-9.
Wells J. M., Brummer, R. J., Derrien, M., Macdonald, T. T., Troost, F., Cani, P. D., Theodorou, V., Dekker, J., Meheust, A., De Vos, W. M., Mercenier A., Nauta, A. & Garcia-Rodenas, C. L. 2017. Homeostasis of the gut barrier and potential biomarkers. *Am J Physiol Gastrointest Liver Physiol,* 312**,** G171-G193.

Appendix

Appendix 1: ddPCR quantification results

Table A1. ddPCR quantification results showing the number of 16S, 18S, and ITS1 copies per µl sample, as well as 16S/18S ratio and 16S/ITS1 ratio for each sample.

	Copies per µl sample			Ratio	
Sample	16S	18S	ITS1	16S/18S	16S/ITS1
1	13 500 000	200	0	67500	
2	8 190 000	31500	210	260	39000
3	15 700 000	130	0	120769	
4	9 290 000	0	0		
5	56 900 000	270	250	210741	227600
6	21 800 000	260	0	83846	
7	31 900 000	3160	840	10095	37976
8	7 850 000	130	0	60385	
9	86 100 000	1990	0	43266	
10	16 900 000	300	0	56333	
11	-	230	0		
12	71 300 000	5540	0	12870	
13	13 700 000	0	85		161176
14	14 800 000	2820	0	5248	
15	7 410 000	19600	360	378	20583
16	321 000 000	88000	0	3648	
17	13 600 000	230	0	59130	
18	26 300 000	160	0	164375	
19	11 300 000	130	0	86923	
20	32 200 000	23200	19200	1388	1677
21	10 200 000	2390	1650	4268	6182
22	19 700 000	0	610		32295
23	7 820 000	11400	530	686	14755
24	5 220 000	11300	0	462	
25	25 600 000	5360	18500	4776	1384
26	30 200 000	750	0	40267	
27	42 200 000	35600	93	1185	453763
28	53 500 000	640	0	83594	
29	40 900 000	6520	0	6273	
30	66 600 000	1560	0	42692	
31	6 240 000	300	690	20800	9043
32	6 490 000	110	340	59000	19088
33	8 290 000	11900	490	697	16918
34	15 300 000	70	0	218571	
35	22 200 000	1320	8500	16818	2612
36	10 300 000	71	0	145070	
37	33 100 000	32600	15600	1015	2122
38	5 510 000	1690	410	3260	13439
39	13 500 000	37	240	364865	56250
40	23 700 000	740	0	32027	
41	11 600 000	90	0	128889	
42	2 860 000	110	0	26000	
43	9 520 000	170	0	56000	

Appendix 2: Fungal OTUs detected in Illumina sequencing

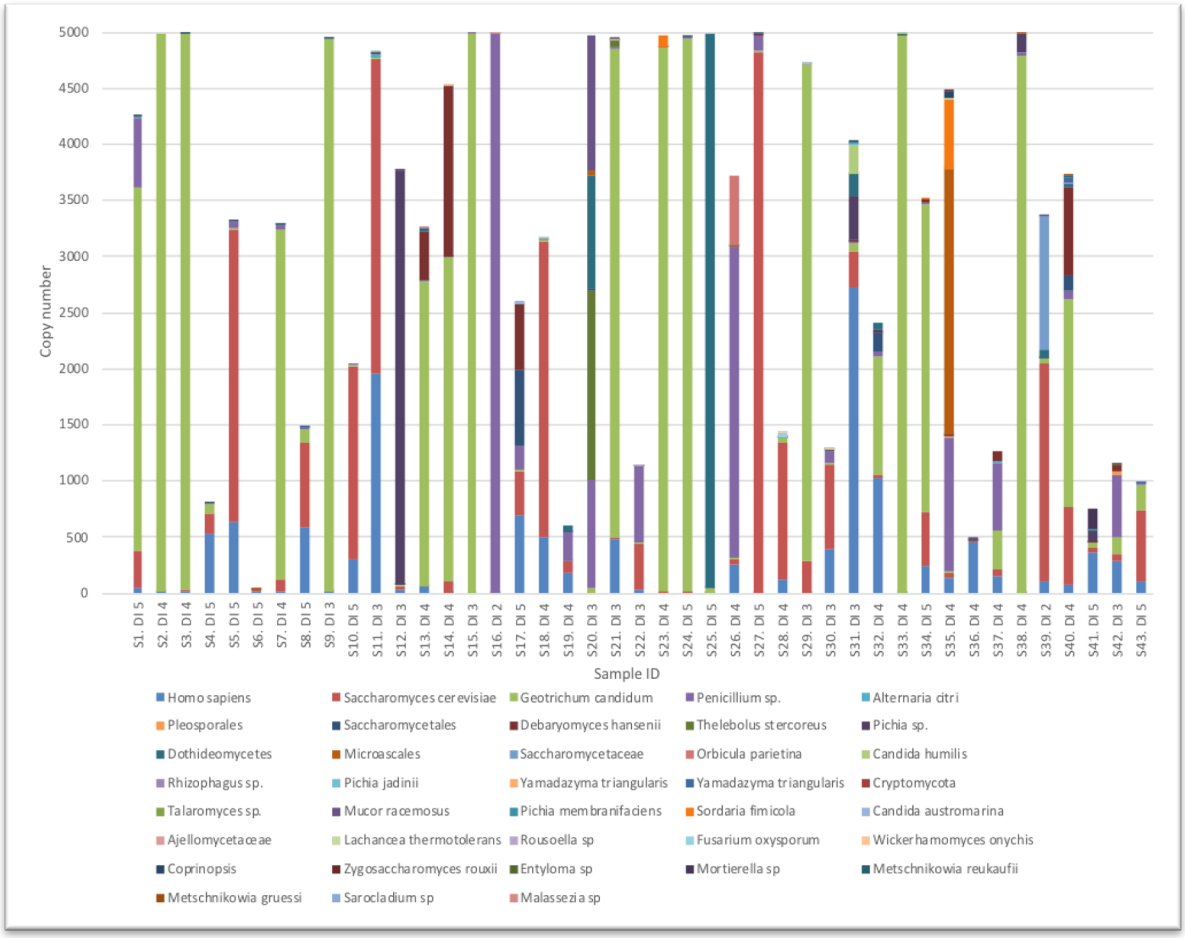

Figure A1. Fungal OTUs detected through Illumina sequencing of the 18S rRNA gene. *Geotrichum candidum (light green), Saccharomyces cerevisiae (red), and Penicillium sp. (purple) were the most prevalent species. Geotrichum candidum was present in all samples, as well as human DNA (Homo sapiens).*

Appendix 3: Gel electrophoresis of LAD template

Figure A2. Gel electrophoresis of the PCR product of LAD template generation. *Samples 20, 22, 26 and 30 produced no visible bands on the gel.*

Appendix 4: Illumina read numbers and LAD signal detection

		Plants 61ºC		Dothideomycetes 39ºC		T. Stercoreus 60ºC		Pichia 39ºC		G. Candidum 56,5ºC		Penicillium 45ºC		Micrococcales 35ºC		Human 56ºC		D.hansenii 48ºC		S. cerevisiae 40ºC	
Sample	DI	Sequencing	LAD signal	Sequencing	LAD signal	Sequencing	LAD signal	Sequencing	LAD signal	Sequencing	LAD signal	Sequencing	LAD signal	Sequencing	LAD signal	Sequencing	LAD signal	Sequencing	LAD signal	Sequencing	LAD signal
1	5	754		1		0		0		3239		613		0		48		1		329	
2	4	12		0		0		0		4976		0		0		10		0		2	
3	4	2		0		0		0		4963		0		0		21		0		6	
4	5	4139		0		0		2		96		1		0		528		0		181	
5	5	1604		0		0		0		5		60		0		640		0		2601	
6	5	4954		0		0		0		4		1		1		10		1		21	
7	4	1697		2		1		0		3123		38		0		20		3		99	
8	5	3508		4		0		0		116		8		0		590		0		755	
9	3	40		4		0		1		4921		0		0		13		1		10	
10	5	2933		0		0		2		14		1		0		299		0		1716	
11	3	128		0		0		2		17		2		0		1951		5		2801	
12	3	1219		0		1		3683		14		1		0		27		2		38	
13	4	1729		25		0		0		2720		0		0		54		436		4	
14	4	462		4		0		2		2890		2		0		1		1519		106	
15	3	3		0		0		1		4980		10		0		2		0		1	
16	2	1		0		0		0		3		4984		0		1		1		0	
17	5	2372		4		0		0		11		215		0		700		588		389	
18	4	1796		0		0		0		8		7		0		494		0		2645	
19	4	4372		51		0		0		5		256		0		181		1		102	
20*	3	25	NA	1017	NA	1693	NA	2	NA	46	NA	962	NA	37	NA	0	NA	0	NA	2	NA
21	3	38		2		64		4		4359		7		0		478		0		17	
22*	3	3852	NA	0	NA	1	NA	0	NA	19	NA	674	NA	6	NA	26	NA	2	NA	407	NA
23	4	24		0		0		0		4857		1		0		8		0		5	
24	5	24		13		0		0		4932		16		0		3		1		8	
25	5	11		4945		0		0		37		1		0		3		0		1	
26*	4	1266	NA	1	NA	0	NA	0	NA	6	NA	2777	NA	3	NA	257	NA	0	NA	51	NA
27	5	15		0		0		0		15		140		1		2		3		4817	
28	4	3490		2		1		1		45		1		0		116		0		1222	
29	3	275		0		0		0		4433		5		0		6		0		276	
30*	3	3701	NA	2	NA	0	NA	0	NA	8	NA	108	NA	0	NA	388	NA	0	NA	764	NA
31	3	866		198		0		387		80		14		1		2730		15		306	
32	4	2582		58		0		34		1051		51		0		1030		1		27	
33	4	16		1		0		0		4967		0		0		6		2		2	
34	5	1485		0		0		1		2736		10		0		236		34		490	
35	4	518		4		0		0		14		1189		2361		132		17		50	
36	4	4517		4		1		1		5		1		0		456		0		11	
37	4	3667		0		0		0		342		609		0		151		79		61	
38	4	13		0		0		166		4782		29		1		2		0		5	
39	2	1633		65		1		8		39		0		0		111		0		1942	
40	4	1270		28		0		0		1860		76		0		72		794		691	
41	5	4230		1		0		93		36		2		0		357		7		57	
42	3	3728		0		0		0		154		560		0		293		60		55	
43	5	3990		0		0		0		222		20		0		104		0		631	

Figure A3. Illumina reads and LAD signal detection. *See explanation on the next page.*

The figure shows both the number of reads from Illumina sequencing, and LAD signals for each probe target in each sample. DI scores of each sample are also given. The fields marked with color mean LAD signal produced. Green – FAM probes, orange – HEX probes, red – ROX probes, blue – CY5 probes.

**no LAD result for this sample (not applicable – NA) because there was no template DNA present in this sample (no band was produced in gel electrophoresis)*

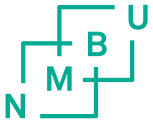

Norges miljø- og biovitenskapelige universitet
Noregs miljø- og biovitskapelege universitet
Norwegian University of Life Sciences

Postboks 5003
NO-1432 Ås
Norway